ACS ES&T Air

pubs.acs.org/estair

Article

Chemical Characterization of Organic Aerosol Tracers Derived from Burning Biomass Indigenous to Sub-Saharan Africa: Fresh Emissions versus Photochemical Aging

Published as part of ACS ES&T Air special issue "Wildland Fires: Emissions, Chemistry, Contamination, Climate, and Human Health".

Adrienne M. Lambert, Cade M. Christensen, Megan M. McRee, Vaios Moschos, Markiesha H. James, Janica N. D. Gordon, Haley M. Royer, Marc N. Fiddler, Barbara J. Turpin, Solomon Bililign,* and Jason D. Surratt*

Cite This: https://doi.org/10.1021/acsestair.4c00206

Read Online

ACCESS | Metrics & More | Article Recommendations | Supporting Information

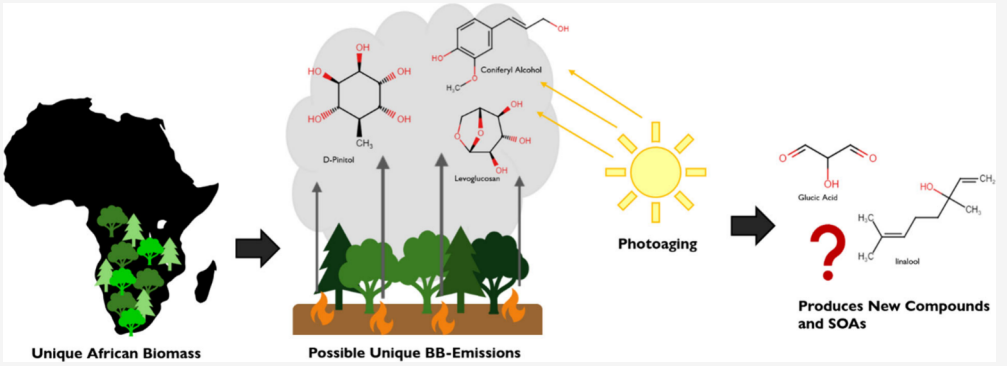

ABSTRACT: Wildfires are increasingly frequent and intense, leading to substantial production of biomass burning (BB)-derived organic aerosol (BBOA). BBOA adversely affects public health and perturbs the climate. Although African fires account for over 50% of worldwide BB-derived organic emissions, few studies have systematically analyzed molecular tracers of BBOA in fresh versus photochemically aged BB emissions representative of African fires. Therefore, by using gas chromatography interfaced to electron ionization quadrupole mass spectrometry (GC/EI-MS), we chemically characterized aerosol filter samples collected from both fresh and photochemically aged BB emissions of six biomass fuels found in Sub-Saharan Africa (*Cordia africana*, *Baikiaea plurijuga*, *Acacia erioloba*, *Colophospermum mopane*, cow dung, and a fuel mixture). BB emissions were generated from a furnace mimicking smoldering combustion and subsequently injected into a humidified laboratory chamber (70% ± 3% RH). Seventeen known BBOA tracer compounds (e.g., levoglucosan, mannosan, coniferyl alcohol, catechol, and palmitic acid) were targeted, quantified, and compared between fresh and photochemically aged BB emissions. Furthermore, total-suspended atmospheric particulate matter (PM) samples collected from Botswana during the fire season were also analyzed by GC/EI-MS. We identified laboratory-generated BBOA constituents that were also found in Botswana PM that could plausibly serve as unique tracers (e.g., D-pinitol) for African BBOA during future field studies.

KEYWORDS: *smog chamber, emission factors, gas chromatography, mass spectrometry, atmospheric oxidation, African fuel, and wildfires*

1. INTRODUCTION

The atmospheric burden of greenhouse gases has substantially increased since the start of the Industrial Revolution in 1760 due to anthropogenic activities.[1−3] Increases in greenhouse gas emissions have accelerated climate change, leading to increasing temperatures and drier conditions. This has resulted in frequent extreme weather events and increases in the frequency and intensity of wildfires, causing substantial amounts of biomass burning (BB)-derived organic aerosol (BBOA) to exist in the atmosphere.[4−6] It is predicted that the contribution of BB to the global greenhouse gas budget will

Received: August 16, 2024
Revised: October 6, 2024
Accepted: October 8, 2024

Table 1. Summary Experimental Conditions for Smog Chamber Combustion Experiments

Expt #	Fuel Type	Sampling Period	Duration Of Sampling (min)	Average Chamber RH (%)[a]	Average Chamber Temperature (C)[b]	Starting SMPS Mass Concn (μg m^{-3})[d]	Mass of Fuel Burned (g)[c]	Total Aerosol Mass on Filter (μg)[e]
1	Sub-Saharan African Fuel Mix	Fresh	11.2	70.25	20.49	1182.5	0.4526	360.00
1	Sub-Saharan African Fuel Mix	Photoaged	21.2	32.35	25.92			490.80
2	*Cordia africana*	Fresh	11.2	73.58	25.61	866.40	0.4174	249.00
2	*Cordia africana*	Photoaged	7.3	30.11	31.12			104.40
3	*Baikiaea plurijuga*	Fresh	10.8	73.6	25.59	1024.6	0.4004	309.00
3	*Baikiaea plurijuga*	Photoaged	11.0	32.74	31.74			111.00
4	Ethiopian Cow Dung	Fresh	10.8	69.81	22.95	497.30	0.3520	159.30
4	Ethiopian Cow Dung	Photoaged	16.0	30.11	29.09			105.75
5	*Acacia erioloba*	Fresh	9.7	32.07	27.59	998.20	0.3155	443.70
5	*Acacia erioloba*	Photoaged	11.0	71.2	21.87			165.60
6	*Colophospermum mopane*	Fresh	11.0	70.26	20.37	786.40	0.4060	233.40
6	*Co1ophosperinuin mopane*	Photoaged	21.2	36.02	26.53			303.60
7*[f]	*Acacia erioloba*	Fresh	10.2	72.35	22.41	1290.0	0.3886	387.00
7*[f]	*Acacia erioloba*	Photoaged	15.3	43.99	27.86			389.07
8*[f]	*Colophospermum mopane*	Fresh	10.5	66.72	22.98	497.20	0.2355	149.16
8*[f]	*Colophospermum mopane*	Photoaged	16.0	30.04	28.65			70.920
9*[f]	*Baikiaea plurijuga*	Fresh	10.3	71.36	23.72	990.20	0.4075	297.06
9*[f]	*Baikiaea plurijuga*	Photoaged	15.5	45.01	22.85			261.09

[a]"Average RH" represents the calculated average relative humidity over the duration of sampling. [b]"Average Temperature" represents the calculated average temperature over the duration of sampling. [c]"Fuel Burn Mass" indicates the initial mass of fuel burned for each experiment. [d]"Starting SMPS Mass Concentration" indicates the mass concentration of aerosol measured by the SMPS at the start of the experiment. [e]"Total Aerosol Mass on Filter" represents the total mass of aerosol particles collected on the filter at the end of each experiment. [f]An asterisk "*" indicates a repeated experiment. These experiments were conducted to replicate the initial chamber combustions.

further increase due to climate change,[3,7,8] and currently up to 75% of the total atmospheric fine aerosol ($PM_{2.5}$) mass loading is from BBOA and black carbon.[9,10]

$PM_{2.5}$ (aerosol particles with aerodynamic diameters of less than 2.5 μm) mass concentrations are rising as wildfires increase and are associated with several adverse health effects.[11−13] Inhalation of $PM_{2.5}$ has been linked to chronic health issues, including inflammation of the lungs, nonfatal heart attacks, aggravated asthma, decreased lung function, lung cancers, and premature death for those with chronic conditions.[14,15] In addition, 600,000 premature deaths that occur annually are associated with the smoke produced by open vegetation burning.[7,16,17]

$PM_{2.5}$ can also alter the radiative balance of Earth's atmosphere directly by scattering and/or absorbing incoming solar radiation and indirectly by changing cloud properties and precipitation.[18] The impact of $PM_{2.5}$ on Earth's radiation balance remains highly uncertain in climate model predictions due (at least in part) to our lack of knowledge of the chemical, optical, and physical properties of $PM_{2.5}$.[18−20] Prior chemical characterization studies on BBOA emissions have focused on Asia,[21−24] Europe,[25−27] and North America;[28−30] however, little is known about the molecular-level composition of African-derived BBOA constituents. Molecular-level chemical identification of BBOA constituents will help improve models, which currently lack emission inventories and types of BBOA constituents from Africa.[31]

While Africa accounts for up to 50% of annual BB carbon emissions produced worldwide, there have been relatively few systematic laboratory studies investigating the chemical and optical properties of BBOA particles from the region.[1,32,33] Botswana is one of many subtropic grassland, woodland, and Mediterranean forest habitat countries in Sub-Saharan Africa that has seen increased wildfires and a lengthening of fire seasons.[34,35] Resolving the molecular-level chemical composition and emissions of BBOA constituents from specific and relevant biomass fuels abundant in a Sub-Saharan African country, such as Botswana, helps to improve predictions of how African BBOA levels affect both regional- and global-scale air quality and climate.

Sample collection and molecular-level chemical analysis can be difficult in the case of BBOA generated from wildfires, because it can be unpredictable and hazardous to sample directly. As a result, systematically generating and characterizing BBOA particles in the laboratory to mimic natural burn events is needed, especially from African-relevant biomass fuels. BB that mimics smoldering fires can be produced by using a tube furnace, where the resulting BBOA and gases can be directly injected into an indoor laboratory smog chamber for sampling and subsequent chemical analysis.[36] Smog chambers allow for a controlled environment to perform experiments for testing the formation of particles and their transformations under different environmental conditions such as humidity, the presence of atmospheric oxidants, and dark and photochemical reactions.[36−38] Fresh BBOA particles are exposed to sunlight during daytime emissions, making it more likely for them to undergo photochemical aging reactions (photoaging), such as photosensitized reactions,[39] heteroge-

https://doi.org/10.1021/acsestair.4c00206
ACS EST Air XXXX, XXX, XXX−XXX

neous oxidation reactions,[40,41] and formation of secondary organic aerosol (SOA) constituents through gas-phase oxidation of volatile BB organic emissions by hydroxyl radical ($^{\bullet}$OH)[38,42−44] and multiphase chemistry of fresh volatile/semivolatile organic compounds.[45−47] Photochemically aged BBOA particles have been demonstrated to be more toxic to humans than when they are freshly emitted to the atmosphere.[48,49] Most BBOA can have atmospheric lifetimes of up to 2−3 weeks, making it important to resolve how the chemical compositions and physiochemical properties of these aerosol particles change as a result of photoaging to improve the accuracy of atmospheric chemistry and climate models.[19,50]

This study helps to address, in part, the gaps in BBOA research described above by examining the chemical composition of freshly generated and photochemically aged BBOA derived from burning well-known and abundant African biomass fuels, especially fuels commonly found in Sub-Saharan Africa (including from Botswana). A total of 17 known BBOA tracer compounds were targeted, identified, and quantified at the molecular level using gas chromatography interfaced to electron ionization quadrupole mass spectrometry (GC/EI-MS) from aerosol filter samples collected from smog chamber experiments. BBOA tracers were compared from both fresh and photochemically aged BB emissions of 6 different African-specific biomass fuels (*Cordia africana*, *Baikiaea plurijuga*, *Acacia erioloba*, *Colophospermum mopane*, Ethiopian cow dung, and a Sub-Saharan African fuel mixture). Fresh BB emissions were generated via a tube furnace that mimicked smoldering conditions (450 °C), and then, the effluent was injected into a humidified smog chamber (initial relative humidity, RH, of 70% ± 3%). Smoldering wildfires produce more organic aerosol, last longer, and are harder to put out than flaming wildfires, making the analysis of smoldering conditions pertinent to this study's experiments.[51] Our study utilizes percent aerosol mass and emissions factors (EFs) to compare compositional differences among the 17 BBOA tracers across the six fuel types examined. We then demonstrate how BBOA tracers from different fuels change after the emissions are photoaged. The results of this study will assist in increasing our understanding of the fresh BBOA tracer emissions in Sub-Saharan Africa and how they chemically transform after atmospheric photochemical aging.

2. EXPERIMENTAL SECTION

Chamber Experiments. The North Carolina Agricultural and Technical State University (NCA&T) 9-m^3 fixed-volume indoor smog chamber facility, previously described in detail by Smith et al.,[36] was used to sample fresh BB emissions (gas-phase species + BBOA). Two sides of the chamber were also equipped with a bank of 32 ultraviolet (UV) lights (Sylvania, F30T8/350BL/ECO, 36 in.), for a total of 64 lamps, to initiate photochemical reactions. A tube furnace (Carbolite Gero, HST120300−120SN) combusted biomass fuels under controlled conditions, and emissions were sent through a cyclone (URG-2000−30ENS-1) with a 2.5-μm cut point before entering the NCA&T smog chamber.[52,53] The chamber mixing fan generated a well-mixed BB mixture for real-time and offline aerosol sampling. Real-time aerosol particle size distributions were measured by a scanning mobility particle sizer (SMPS, TSI, Inc.), which is composed of a cylindrical differential mobility analyzer (DMA, TSI, Inc., Model 3080) coupled to a condensation particle counter (WCPC, TSI, Inc., Model 3788).

Nine chamber experiments were conducted, where fresh BB emissions were transferred into a prehumidified (∼65−75% RH) chamber (Table 1). By flowing particle-free air through a bubbler filled with 400 mL of deionized water (American Society for Testing and Materials (ASTM) type II water), the chamber was humidified.[54] Temperature and RH during the chamber were measured using a Fisherbrand Certified Traceable Digital Hygrometer and Thermometer. The chamber was cleaned between experiments by continuously flushing the chamber for 2−3 days with zero air and turning on UV lights. Before each experiment was started, the cleanliness of the chamber was assessed through SMPS measurements. Chamber aerosol mass concentrations during experiments typically ranged from 600 to 1000 μg m^{-3} following combustion. After completion of each experiment, we flushed the chamber by flowing clean air through it for over 24 h. This allowed us to obtain <2 μg m^{-3} before our next chamber experiment. While ideally this would be near the detection limit of our SMPS system, we believe that <0.3% of background aerosol mass concentration in the chamber is acceptable.

The Sub-Saharan African biomass fuels burned during this study were directly obtained from the continent, but specifically from Sub-Saharan Africa, and included the following: *Cordia africana* (wanza), *Baikiaea plurijuga* (mukusi), *Acacia erioloba* (mokala), *Colophospermum mopane* leaves (mopane), Ethiopian cow dung (cow dung), and a Sub-Saharan African fuel mix consisting of the aforementioned fuels as well as some additional Botswana-relevant fuels that included *Pennisetum setaceum* (savannah grass), *Acacia abyssinica* (acacia), *Peltophorum africanum* (mosetlha), *Olea europaea* (wild olive), and *Eucalyptus camaldulensis* (eucalyptus). Details of these fuels, including their species characteristics and locations in Africa, are summarized by Moschos et al.[53] Cow dung was the only nonplant biomass fuel used, but is still relevant to this study as it is a common household fuel used for cooking and heating.[55] All biomass fuels were collected in Ethiopia and Botswana and immediately wrapped in aluminum foil after they were dried in the sun. Once the aluminum foil-wrapped fuels arrived to NCA&T, they were kept in the fume hood to stay dry. No mold growth or rotting was observed before burning the fuels.

All combusted biomass fuels were dried by placing them under a fume hood, and the resulting moisture content of each fuel that was measured at New Mexico Tech University was typically <10% (Moisture Analyzer PCE-MA 50X). The biomass fuels were sourced from the woody portions of the plant except for mopane leaves, which were the leafy portion of the plant, and cow dung that was sourced from cow dung cakes produced in Ethiopia. To prepare the woody fuels for burning, the outer layer of bark was removed from the fuel to ensure uniform fuel composition and consistency between experiments.

During each experiment, ∼0.30−0.45 g of biomass (see Table 1) was burned in the tube furnace for 10 min at a constant temperature of 450 °C to achieve smoldering conditions. In order be considered smoldering conditions, the experiments needed at modified combustion efficiency (MCE) between 65−85%, and 450 °C maintains an MCE in this range.[56] Smoldering conditions are ideal for BB experiments because in comparison to flaming fires smoldering fires have more BrC, $PM_{2.5}$, and complex organic emissions.[57−60] Furthermore, smoldering fires are the most persistent type of

https://doi.org/10.1021/acsestair.4c00206
ACS EST Air XXXX, XXX, XXX−XXX

combustion because it is easier to ignite but more difficult to suppress than flaming combustion.[61] The fire-average modified combustion efficiency (MCE) was less than 0.85 for all the experiments,[62,63] resulting in organic-rich emissions of $PM_{2.5}$.[53] The MCE was used to determine if the fire stage is flaming- or smoldering-dominating conditions, and our MCE values were consistent with smoldering burn conditions which have MCE values of approximately 0.8 or less.[64,65] During the burning of each biomass fuel, particle-free zero-air from a clean-air generator (Aadco Instruments, 747−30) was passed over the plume of combusted material produced by the furnace and directed into the chamber for 10 min at a flow rate of 10 L min^{-1}, which is consistent with the cyclone's (URG-2000−30ENS-1, URG, Inc.) flow rate requirements for sampling $PM_{2.5}$. After the completion of each burn, the chamber was allowed to become well-mixed for ∼20 min. The latter was confirmed by stable aerosol volume concentrations measured in real-time by the SMPS.

There were two different sampling periods, fresh and photoaged, that were conducted for each biomass fuel, including the following: Experiment #1 for the Sub-Saharan African Fuel Mix, Experiment #2 for wanza, Experiment #3 for mukusi, Experiment #4 for cow dung, Experiment #5 for mokala, and Experiment #6 for mopane (Table 1) (two filters collected per experiment). In addition, replicate experiments were conducted for 3 of the biomass fuels (mopane, mukusi, and mokala) (see SI Section S1 for details and Table 1), and these fuels were chosen because of their prevalence in Sub-Saharan Africa.[53] Further details of these replicate experiments can be found in Section S1 of the Supporting Information (SI).

Sampling of fresh emissions took place right after the aerosols became well-mixed in the chamber (as determined by SMPS when volume concentrations stabilized). The aerosols were collected onto Teflon filters (Tisch Scientific, SF18040; 47 mm diameter, 2-μm pore size, 38 mm aerosol collection diameter) for a duration of 10 min at 30 L min^{-1}. The chamber was then left for ∼3 h to allow other aerosol measurements to be made (e.g., brown carbon (BrC) measurements recently published)[53] before the UV lights surrounding the chamber were turned on to initiate photochemical aging for ∼2 h. After this 2-h period, filter sampling of the photochemically aged emissions was initiated and lasted for 15 min at a flow rate of 30 L min^{-1}. Notably, due to our lack of detailed gas-phase chemical measurements, we were unable to estimate the $^{\bullet}OH$ radical levels (and thus equivalent atmospheric aging days) during this phase of the experiment. This is one major limitation of our study.

During the aerosol sampling of fresh emissions, the chamber had an RH that of ∼70−74% and temperature of 20.4−27.6 °C. The chamber during aerosol sampling of photoaged emissions had an RH of ∼30−36% and a temperature of 25.9−31.7 °C. The increase in temperature and decrease in RH between sampling periods was due to the UV lights changing the conditions in the chamber during the photoaged sampling, mirroring the changes in atmospheric conditions that occur during the daytime.[66,67] While some NO_x is produced from combustion of each fuel (i.e., 52, 30, 22, 30, 28, and 130 ppbv from the fuel mixture, wanza, mukusi, cow dung, mokala, and mopane, respectively), no additional NO_x was added to the chamber, and negligible levels of ozone were produced by either combustion or photolysis.[54]

Teflon filters collected during the fresh and photoaged sampling periods were securely packaged in Petri dishes and wrapped in aluminum foil (to prevent further photochemical reactions) before they were frozen under dark conditions in a −20 °C freezer. All filters were weighed before and after aerosol collection to obtain the mass of aerosol collected on each filter. These filter samples were transported from NCA&T University to the University of North Carolina at Chapel (UNC) in coolers with blue ice for extraction and chemical analysis. Filter samples were only in the coolers for 90 min, which is roughly the transport time by vehicle to UNC from NCA&T University. Upon arrival to UNC, filters were immediately removed from coolers and placed in a −20 °C freezer at UNC.

Ambient Aerosol Samples Collected from Botswana. In addition to the chamber experiments, ambient aerosol samples were collected from two locations during a field campaign in Botswana for the purpose of comparing the laboratory-generated BBOA emissions to actual atmospheric samples that were influenced by BBOA. Total suspended PM samples were collected during the 2022 wintertime fire/heating season from June 24 to July 21 in Gaborone, the Capital of Botswana, and at the Botswana International University of Science and Technology (BIUST) weather station in Palapye. The two sampling sites were chosen based on their campaign-average PM loadings, with the Gaborone site having a high PM loading of ∼150 $\mu g\ m^{-3}$, and the BIUST site having a lower PM loading of approximately ∼10 $\mu g\ m^{-3}$.[53] Using a portable pump with a filter holder (Savillex, 401−21−47−30−21−2) with no cyclone attached and containing 47 mm Teflon filters, 10 total suspended PM (TSP) samples were taken, one at a time, in either 12- or 24-h sampling periods. Either a piston (Rocker, 800, 23 L min^{-1}) or diaphragm pump (SKC Ltd., Leland Legacy, ∼10 L min^{-1}) was used. The 12-h sampling periods were either during the daytime or nighttime. The average temperature was 21 °C, and an average RH was 50%. The ambient aerosol filters were weighed before and after sampling and kept at −20 °C while on site. For transport to NCA&T in the US, all filters were removed, wrapped in tinfoil, and then kept again at −20 °C at NCAT before they could be analyzed by GC/EI-MS. The extraction and chemical analysis processes were identical for ambient aerosol filters and chamber filters.

Filter Extraction and Sample Preparation. To prepare for filter extractions, Teflon filters were first defrosted by sitting at room temperature for ∼20 min. The filters collected from the chamber experiments had polypropylene support rings that were removed using a filter punch and tweezers. The filters were then placed into prelabeled and precleaned 20 mL scintillation vials. These vials were filled with approximately 20 mL of Optima LC/MS grade methanol. The scintillation vials were then sealed with polytetrafluoroethylene (PTFE) caps, wrapped thoroughly in Teflon tape, and sonicated for one 20 min interval and one 25 min interval. The water in the sonicator was drained and then refilled between intervals to control the temperature of the water bath inside the sonicator. After the completion of sonication, extracts in the 20 mL scintillation vials were filtered using LC/MS certified syringe filters (0.2-μm pore size, poly(ether sulfone), PES, membrane, Agilent) attached to a 10 mL glass syringe to remove any large or insoluble particles (e.g., soot) or filter fibers that could disrupt chemical analysis by GC/EI-MS. The extracts were drawn up by the 10 mL syringe, the needle was capped and then unscrewed from the syringe, and then a PES syringe filter was screwed onto the syringe in its place before the extract in

https://doi.org/10.1021/acsestair.4c00206
ACS EST Air XXXX, XXX, XXX−XXX

the syringe was transferred into a new 20 mL precleaned scintillation vial. One quarter of the filtered extract was then used for GC/EI-MS analysis presented in this study (the remaining three-quarters were used for BrC molecular analysis[53]). Methanol was chosen as the solvent of choice because methanol extraction resulted in the clean chromatographic backgrounds and produced a high extraction efficiency of a wide array of organic molecules contained in the aerosol. The literature has also cited methanol extraction for analysis of organic compounds resulting from biomass burning, with reports of >90% of compounds from BBOA being extractable in methanol.[68−70]

The filtered methanol extracts were dried at room temperature using a high-purity N_2 evaporator (NI HP300 from Airgas). Because of the low reconstitution volume of the filter extracts, the samples were dried down to approximately 150 μL, transferred into a 250-μL glass insert, and then dried to completion. This was done to prevent evaporative losses of the BBOA constituents. When the filter extracts in the glass inserts completely evaporated, the glass inserts were put into 2 mL amber screwcap HPLC vials, and then the dried solution was reconstituted with 25 μL of anhydrous 99.8% pyridine using a 100-μL Hamilton gastight syringe. The HPLC vials were capped immediately, and the vials were carefully rotated to make sure all of the dried particles were in solution. After all the samples were reconstituted in the HPLC vials with pyridine, a 1 mL ampule of N,O-Bis(trimethylsilyl)-trifluoroacetamide (BSTFA) with trimethylchlorosilane (TMCS) was opened, and 50 μL was immediately added to each vial using a 100-μL Hamilton gastight syringe in order to trimethylsilylate the BBOA constituents before GC/EI-MS analyses. The vials were immediately capped with 9 mm slitted screw caps and then heated at 70 °C for 1 h. The heated vials were then analyzed within 24 h by using GC/EI-MS (see the subsequent section below).

Trimethysilyation is needed to ensure that BBOA constituents, which typically contain hydroxyl and carboxyl functional groups, are amendable to GC/EI-MS analysis.[71] Trimethylsilylation replaces the hydrogen in these functional groups to add trimethylsilyl groups (TMS). The addition of TMS groups to our targeted BBOA constituents increases their volatility by lowering the boiling point. This allowed the GC system to vaporize these targeted BBOA constituents so that they could be analyzed by EI-MS.

GC/EI-MS Analysis. The GC/EI-MS analysis method used in our study was previously described in detail by Surratt et al.[72] Briefly, 1-μL aliquots of each derivatized filter extract were injected in spitless mode onto a GC (Agilent, 8890) interfaced to a quadrupole mass spectrometer (Agilent, 5977B MSD) equipped with an EI source. BBOA compounds were separated by an Agilent HP-5MS Ultra Inert fused-silica capillary column ((5%-phenyl)-methylpolysiloxane, 30 m × 0.25 mm inner diameter, 0.25-μm film thickness) using a 65.17 min temperature gradient scheme. The GC carrier gas was helium (Airgas, Ultra High Purity) with a flow rate of 0.8 mL min^{-1}. Both the GC inlet and detector temperatures were held at 250 °C. The GC/EI-MS raw data were analyzed with MassHunter Workstation Qualitative Analysis 10.0 software (Agilent) with the purpose of identifying and quantifying the 17 target analytes.

Seventeen target analytes were selected based on BBOA tracers that were identified in previous work[7,73−75] and compounds that displayed high abundance in chamber-generated BBOA. The targeted BBOA constituents were as follows: lactic acid (Sigma, 99%), glycolic acid (Sigma, 99%), glycerol (Sigma, 99.5%), catechol (Sigma, 99%), resorcinol (Sigma, 99%), 4-methylcatechol (Sigma, 95%), hydroquinone (Sigma, 99%), pyrogallol (Sigma, 98%), tyrosol (Sigma, 98%), mannosan (Spex, 1000-ppm), levoglucosan (Sigma, 99%), hydroxytyrosol (Fisher, 97.5%), D-pinitol (Sigma, 95%), coniferyl alcohol (Sigma, 98%), scopoletin (Sigma, 98%), palmitic acid (Sigma, 99%), and stearic acid (Sigma, 98.5%). All of the compounds and their associated retention times (RTs) were confirmed with these authentic standards. Peak areas of the 17 compounds (taken from the unique/abundant fragment ions for each compound, see SI Table S1) in each of the samples (the fresh and photoaged emissions of ambient and laboratory-generated aerosol samples) were recorded. As will be described below in the Results and Discussion section, lactic acid was not included in our BBOA analysis due to being present in blanks. Thus, our final targeted list of BBOA constituents was narrowed down to 16 species. By using calibration curves created for each targeted BBOA constituent, the percent aerosol mass for each target analyte was calculated using the total mass of aerosol on the filter. Details for generating GC/EI-MS calibration curves and their application for deriving aerosol mass fractions are provided in Section S2 of the SI. In addition, details of our GC/EI-MS quality assurance steps and quality controls are provided in the SI, which includes the following: (1) GC/EI-MS analysis of filters collected from chamber air backgrounds, solvent blanks, and filter blanks (Section S3); (2) GC/EI-MS analysis of individual standards versus standards in a mixture (Section S4); (3) determination of reconstitution volumes of derivatizing reagents for GC/EI-MS analysis (Section S5); (4) assessment of reproducibility of GC/EI-MS results (Section S6); and (5) filter extraction efficiencies and recoveries of targeted BBOA constituents measured by GC/EI-MS (Section S7). The authentic standards used for the GC/EI-MS calibration curves and to verify the compounds in the chamber experiment chromatograms were also used to determine the extraction efficiencies for the target analytes. The GC/EI-MS limits of detection (LOD) and limits of quantification (LOQ) were calculated for each of the target compounds identified in the BBOA samples collected from burning each of the fuels. LODs and LOQs were calculated using calibration curve derived standard deviations (see Table S2 LODs/LOQs of each compound).

Calculation of Emission Factors (EFs) for Targeted BBOA Constituents. EFs, which relate the amount of a pollutant released into the air to the mass of fuel burned, were calculated for the fresh BB emissions of our targeted BBOA constituents. To calculate EFs for each BBOA constituent in the fresh emissions, the starting SMPS mass concentration ($\mu g\ m^{-3}$) measured during each chamber experiment was multiplied by the chamber volume, which was constant at 9 m^3. This provides the total mass of fresh BBOA in the chamber during each experiment in units of μg prior to any chamber dilution that results from aerosol sampling. The total mass of fresh BBOA in the chamber is multiplied by the aerosol mass fraction of each targeted compound (this value is in decimal form), which gives the total mass of each targeted BBOA compound in the chamber in μg. Finally, the total mass of each BBOA compound is divided by the total mass of the fuel burned in kg, which provides the EF for each BBOA compound from the respective fuel sample in $\mu g\ kg^{-1}$. The

https://doi.org/10.1021/acsestair.4c00206
ACS EST Air XXXX, XXX, XXX−XXX

EFs calculated using this method were then converted to units of mg kg^{-1} to be comparable to past studies.[73] The data obtained were used to compare the fresh versus photoaged emissions, laboratory-generated aerosols versus ambient aerosols, and the relationships between the different fuels. To calculate EFs, we assume that the fuel in the furnace burned completely, all BB fuel particle emissions entered the chamber (i.e., we neglect tubing wall losses between the furnace and chamber), and the chamber wall losses in the first few minutes (i.e., when the mass loading was estimated by the SMPS) are negligible.

Chemicals. The chemicals used for the extraction, reconstitution, and derivatization processes were all LC/MS-certified methanol (Fisher Optima). In addition, we used anhydrous 99.8% pyridine (Sigma), and BSTFA (Sigma) with 1% TMCS (Sigma). The standard chemicals used for the 17 targeted BBOA compounds are listed in Table S3 in the SI.

Determination of Analytical Uncertainty. To test the analytical reproducibility of the GC/EI-MS method, mixtures of authentic standards were prepared the same way as the calibration curves and samples described previously. The mixture was injected 3 consecutive times to obtain an average response and standard deviation for each analyte. This was done on 3 separate days, yielding a total of 9 individual responses for each analyte. For this test, the pooled standard deviation (s_{pooled}) for all analytes was calculated with the following formula

$$s_{pooled} = \sqrt{\frac{\sum s_i^2}{N}}$$

where s_i represents the standard deviation of a given analyte on a given day, and N represents the number of data points, which in this case would be $3(A)$ where 3 represents the number of days, and A is the number of analytes measured on each day. The analytical uncertainty was calculated by

$$\frac{s_{pooled}}{\bar{x}} \times 100 = \text{Analytical Uncertainty (\%)}$$

The average of all peak areas for all analytes on all 3 days is represented by $\bar{x}$. The calculated uncertainty was 5.0% and is represented in the error bars for Figures 2−9 below.

3. RESULTS AND DISCUSSION

QA/QC Testing to Confirm BBOA Marker Compounds for Use during Burn Experiments. For the 6 African biomass fuels burned under smoldering conditions in the laboratory, 17 targeted BBOA compounds were initially investigated in primary BBOA generated from these fresh BB emissions by using GC/EI-MS extracted ion chromatograms (EICs) associated with known and unique fragment ions (Table S1). To ensure that these fresh and targeted BBOA marker compounds were accurately identified in the aerosol samples collected, and not a result of chamber background, the EICs of each target compound were compared to the averaged chromatogram of 2 chamber filter blanks. The chamber blank is a collection of background air with no active burn occurring, on the same type of Teflon filter used during the burn experiments. As an example, Figure S1 in the SI shows the EICs of 4 (i.e., lactic acid, levoglucosan, D-pinitol, and stearic acid) of the 17 targeted BBOA marker compounds from burning the 6 African biomass fuels versus the EICs of the same fragment ions associated with these 4 BBOA marker compounds in the chamber filter blank. EICs of m/z 117, 204, 260, and 341 were used to compare lactic acid (the earliest eluting compound from GC/EI-MS), levoglucosan, D-pinitol, and stearic acid (the latest eluting compound from GC/EI-MS), respectively, in the primary BBOA samples collected from all 6 smoldering burns versus a chamber blank. From the sets of EICs shown in Figures S1b-S1d, the chamber blank has chromatographic peaks for these targeted BBOA tracers (i.e., levoglucosan, D-pinitol, and stearic acid) that are near zero in signal compared to their chromatographic peaks found in the primary BBOA samples generated from burning of the 6 biomass fuels. This emphasizes that levoglucosan, stearic acid, and D-pinitol are not a result of the smog chamber background and that these targeted BBOA compounds are present in the primary BBOA samples. From the EICs shown in Figure S1a, the chamber blank has a chromatographic peak of lactic acid that is much larger than that of the primary BBOA samples generated from burning the 6 fuels. As a result, lactic acid was not included in our further analyses of the fresh or aged BBOA samples collected from the chamber studies. When analyzing the background in comparison to the other 13 compounds, the chromatogram for the chamber blank was near detection limit for these remaining BBOA constituents. Thus, a total of 16 BBOA constituents are targeted in our analyses.

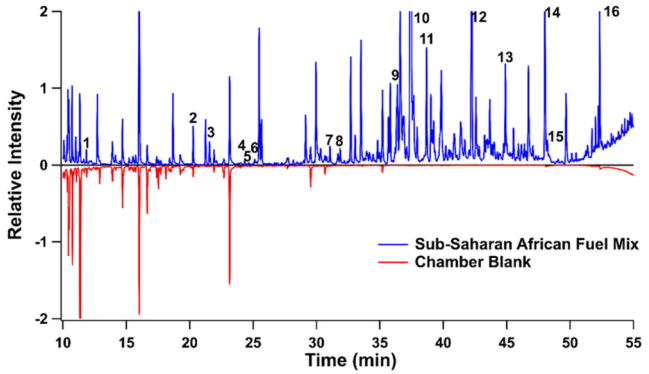

Figure 1. GC/EI-MS TIC of the fresh (primary) BBOA sample collected from burning the Sub-Saharan African Fuel Mix (blue) vs the GC/EI-MS TIC of a chamber blank (red). The chromatograms are magnified to depict a better definition of peaks. The target compounds are labeled 1−16 (1−glycolic acid, 2−glycerol, 3−catechol, 4−resorcinol, 5−methylcatechol, 6−hydroquinone, 7−pyrogallol, 8−tyrosol, 9−mannosan, 10−levoglucosan, 11−hydroxytyrosol, 12−D-pinitol, 13−coniferyl alcohol, 14−scopoletin, 15−palmitic acid, 16−stearic acid). The compound lactic acid (RT ∼ 11.35 min) and many of the other peaks eluting before 20 min are associated with the blanks and not with the burn samples. Notably, most compounds eluting after 24 min are unique BBOA marker compounds not found in the filter blanks/chamber background. A full list of compounds either identified by authentic standards or suggested from the NIST EI-MS library that are a part of the chamber/filter backgrounds is provided in Tables 2, 3, S5, and S7. No chromatographic peaks are shown before 7.5 min due to the solvent delay needed for GC/EI-MS, and none of the target BBOA compounds have chromatographic peaks before 10 min.

To further substantiate the detection and use of the remaining targeted BBOA compounds, Figure 1 shows the entire total ion chromatogram (TIC) of the Sub-Saharan African Fuel Mix overlaid with the TIC from a chamber blank experiment. Aside from the background of lactic acid, the chamber blank signal remains near zero for the remaining 16 targeted BBOA compounds in primary BBOA generated from

https://doi.org/10.1021/acsestair.4c00206
ACS EST Air XXXX, XXX, XXX−XXX

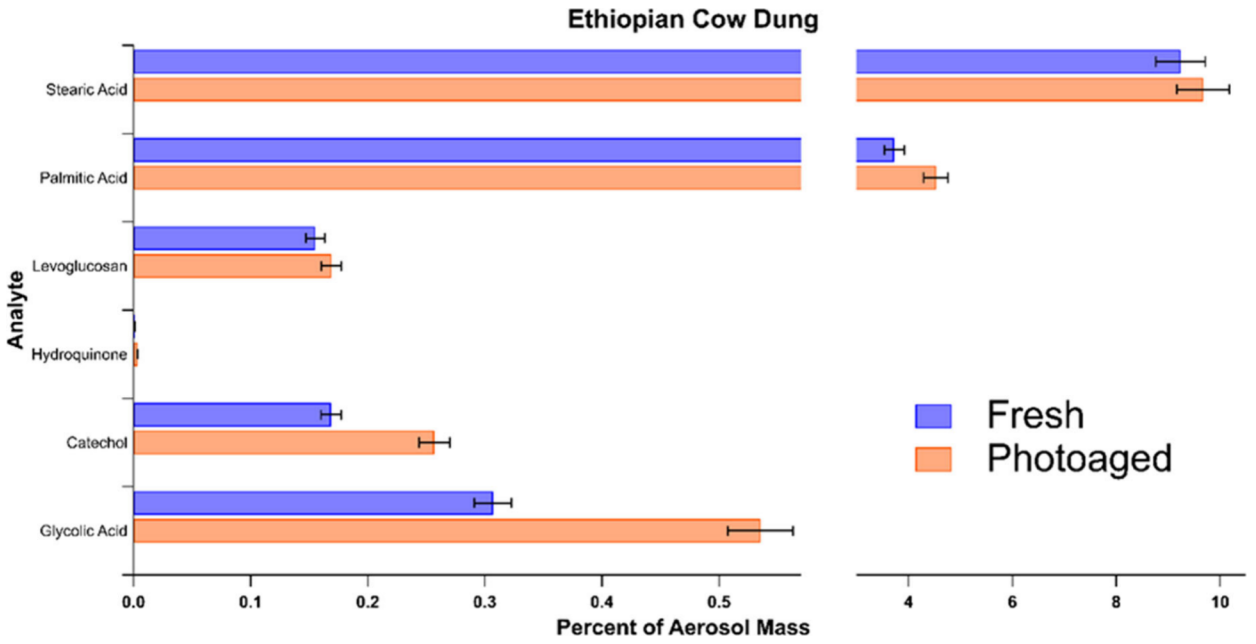

Figure 2. Comparisons of the aerosol mass fractions (in %) of targeted BBOA marker compounds found in both the fresh and photoaged BBOA emissions from cow dung. Error bars represent calculated uncertainty in the analytical method.

Table 2. Identified Targeted Compounds in Fresh BBOA Samples Were Confirmed with Authentic Standards[a]

		Fuel Name					
Compound Name	RT (min)	Mopane	Mukusi	Wanza	Ethiopian Cow Dung	Sub-Saharan African fuel mix	Mokala
Glycolic Acid	11.8	X	X	X	X	X	X
Glycerol	20.3	X	X			X	X
Catechol	21.6	X	X	X	X	X	X
Resorcinol	24.3		X	X		X	X
4-Methylcatechol	24.7	X	X	X		X	X
Hydroquinone	25.1	X	X	X	X	X	X
Pyrogallol	31.0					X	
Tyrosol	31.9					X	
Mannosan	36.6	X				X	X
Levoglucosan	37.4	X	X	X	X	X	X
Hydroxytyrosol	39.3						
D-Pinitol	42.2	X				X	
Coniferyl Alcohol	44.9		X	X		X	X
Scopoletin	47.6					X	
Palmitic Acid	48.0	X	X	X	X	X	X
Stearic Acid	52.3	X	X	X	X	X	X

[a]An X symbol denotes the detection of the targeted BBOA constituent in the fresh aerosol emissions.

burning the Sub-Saharan African Fuel Mix. This QA/QC result was observed for all the other chamber experiments.

BBOA Marker Compounds Identified in Primary Emissions from Smoldering Burns. The GC/EI-MS analysis of the fresh BBOA samples collected from burning the six African biomass fuels confirmed either the presence or the absence of the 16 targeted BBOA marker compounds in each experiment (Table 2). Several targeted BBOA marker compounds, including glycolic acid, catechol, hydroquinone, levoglucosan, palmitic acid, and stearic acid, were present in all six of the experimental burns (including the 3 replicate experiments, Experiments # 7−9 in Table 1 and Table S4). This was expected, as many of these organic compounds are well-established molecular tracers used to identify the presence of BB emissions in the atmosphere or have been frequently identified in wildfire BB emissions.[74−78] Notably, levoglucosan is derived from the pyrolysis of cellulose and hemicellulose, which are found in high concentrations in the cell walls of all Tracheophyte plants (all vascular plants).[79] Palmitic and stearic acids are long-chain fatty acids derived from oils and waxes that plants use in their membranes and cuticles, as well as for cellular transport and communication.[80] Catechol is formed from the oxidation of phenols,[81] and phenols play a role in plant colors, along with their defense mechanisms against predators, pathogens, and radiation.[82,83] Many phenols are derived from the lignin in plants, making the origins of catechol akin to coniferyl alcohol and resorcinol,[84] which is described below. Lignin makes up the structural components of the plant cell wall; specifically, in the green stem or woody potions of a plant.[85] Hydroquinone can be derived through the pyrolysis of phenols found in plants,[86] or it can naturally exist in plants as secondary metabolites.[87] Glycolic acid is formed

https://doi.org/10.1021/acsestair.4c00206
ACS EST Air XXXX, XXX, XXX−XXX

Table 3. Tentatively Identified Compounds (as Their TMS Derivatives) in Fresh BBOA by the NIST Library

Compound Name	RT (min)	NIST Identity Probability (%)	Present In Fuel					
			Mopane	Mukusi	Wanza	Cow Dung	Sub-Saharan African Fuel Mix	Mokala
Diethylene glycol	18.67	73.0		X			X	X
Butanedioic acid	21.56	88.0	X	X	X	X	X	X
Dodecanoic acid	34.80	91.9		X	X			
Sinapaldehyde	46.73	95.7		X	X		X	X
trans-Sinapyl alcohol	49.68	96.4		X	X		X	X

Table 4. Emission Factors (EFs) of Confirmed BBOA Tracer Compounds (Ordered by Increasing RT) from Burning African-Relevant Biomass in mg of Compound per kg of Fuel Burned (mg kg^{-1})

BBOA Tracer Compound Name	EFs of BBOA Tracer Compounds from Burning Each Fuel (mg kg^{-1})[a]					
	Mukusi	Cow Dung	Mokala	Mopane Leaves	Wanza	Sub-Saharan African Fuel Mix
Glycolic Acid	55.7	39.1	41.9	37.6	50.5	33.5
Glycerol	6.70	ND[b]	4.17	5.73	ND[b]	4.93
Catechol	31.9	21.5	18.1	20.4	30.4	19.5
Resorcinol	13.5	ND[b]	7.60	ND[b]	8.85	8.00
4-Methylcatechol	13.5	ND[b]	9.41	10.6	13.3	9.71
Hydroquinone	3.56	ND[b]	NQ[c]	ND[b]	NQ[c]	NQ[c]
Pyrogallol	ND[b]	ND[b]	ND[b]	ND[b]	ND[b]	17.6
Tyrosol	ND[b]	ND[b]	ND[b]	ND[b]	ND[b]	8.05
Mannosan	ND[b]	ND[b]	106	15.6	ND[b]	27.7
Levoglucosan	1090	19.7	2170	178	536	758
Hydroxytyrosol	ND[b]	ND[b]	ND[b]	ND[b]	ND[b]	ND[b]
D-Pinitol	ND[b]	ND[b]	ND[b]	358	ND[b]	64.0
Coniferyl Alcohol	315	ND[b]	66.6	ND[b]	262	95.0
Scopoletin	ND[b]	ND[b]	ND[b]	ND[b]	ND[b]	60.0
Palmitic Acid	480	473	318	389	467	360
Stearic Acid	956	1180	638	749	918	699

[a]Each value has an inherent 5.0% uncertainty based on the pooled standard deviation of replicate injections across several days. [b]ND − Compound is not detected. [c]NQ − Compound is detected but cannot be quantified due to LOQ.

through the •OH oxidation of abietic acid, which is a primary component in plant resins.[88,89]

Besides the BBOA marker compounds discussed above, which were found in aerosols generated from all burning experiments, other BBOA compounds were unique to only a few of the fuels. Resorcinol and coniferyl alcohol were both present in mukusi, wanza, mokala, and the Sub-Saharan African fuel mix. They were missing from aerosol samples generated from burning leaves of mopane and cow dung. This is due to resorcinol and coniferyl alcohol both originating from the lignin in plants.[90,91] Mopane leaves lack the structure to have high amounts of lignin, and cow dung is not plant matter (no cell walls). D-Pinitol was only present in mopane leaves and the Sub-Saharan African fuel mix emissions. The cow dung fuel has the smallest number of targeted BBOA compounds, with only glycolic acid, catechol, hydroquinone, levoglucosan, palmitic acid, and stearic acid present. This is due to many of the targeted BBOA marker compounds being associated with primary emissions from burning plant biomass, and the plants in cow dung were broken down through digestion leaving only undigested material for tracers.[92] A few of the targeted BBOA compounds, such as pyrogallol, tyrosol, and scopoletin, are present only in fresh BBOA aerosols collected from burning the Sub-Saharan African fuel mix. This is due to the fuel mix not only containing the six individual fuels examined in this study but also being composed of five additional fuels relevant to Sub-Saharan Africa that included savannah grass, acacia, mosetlha, wild olive, and eucalyptus. Notably, Moschos et al. previously observed scopoletin in primary BB emissions from solely burning wild olive (which was not examined alone in our present study).[53]

As shown in Figure 1 above, besides the 16 of the 17 targeted BBOA tracer compounds being detected, additional BBOA compounds were detected in high abundance in multiple GC/EI-MS TICs from the biomass fuels examined in this study. Table 3 summarizes the tentatively identified BBOA compounds found during nontargeted GC/EI-MS analysis of all biomass fuels by using the NIST Library associated with the software Qualitative Analysis of MassHunter Acquisition Data 10.0. The identity of these compounds is only tentative due to the lack of confirmation with available authentic standards. This table lists the tentative BBOA compound name, RTs, NIST identity probability, and the presence or absence of the tentative BBOA compound in each fuel. All BBOA compounds listed in this table have a NIST identity probability of at least 73% and were the top compound on the predicted list. The tentatively identified BBOA compounds in the TICs generated from GC/EI-MS analyses of aerosols from each fresh burn were diethylene glycol, butanedioic acid (succinic acid), dodecanoic acid (lauric acid), sinapaldehyde, and *trans*-sinapyl alcohol. Butanedioic acids are present in BBOA samples collected from burning all six fuels. Butanedioic acid has been shown to be an abundant organic compound found in BB emissions from Asia.[93−95] Mukusi had every tentatively identified BBOA compound listed in Table 3 present in its TIC, whereas mopane leaves and cow dung only contained butanedioic acid. This could be due to the differences in the makeup of dung

https://doi.org/10.1021/acsestair.4c00206
ACS EST Air XXXX, XXX, XXX−XXX

and leafy green matter versus the other woody fuels. Diethylene glycol was the only compound that was not present in wanza but present in the Sub-Saharan African fuel mix, mokala, and mukusi, suggesting a similarity between these fuels. The compounds tentatively identified and listed in Table 3 could be possible BBOA tracers specific to certain families of plants or regions in the continent of Africa and should be evaluated in-depth in future studies. Sinapaldehyde and *trans*-sinapyl alcohol were identified as being present in mukusi, wanza, mokala, and the Sub-Saharan African fuel mix. Sinapyl alcohol is a known lignin unit found in plants and is often identified with coniferyl alcohol in BB emissions, a proposed wood burning tracer.[75,96,97] Sinapaldehyde is known to form due to the breakdown of sinapyl alcohol during lignin pyrolysis and has also been demonstrated in the literature as being a major light-absorbing organic compound present in BB emissions.[52,53,98]

Emission Factors (EFs) of Confirmed BBOA Tracer Compounds from the Six Biomass Fuels Examined. Table 4 summarizes the EFs in milligrams of the BBOA tracer compound measured per kg of fuel burned (mg kg^{-1}) of the target BBOA compounds in each of the six fuels. For all of the fuels examined, except for cow dung and mopane leaves, levoglucosan had the highest EF (20−2170 mg kg^{-1}) of the 16 targeted compounds, which is consistent with prior studies.[73,74,77] The EFs for levoglucosan can most easily be compared to the EFs found in other studies. EFs for particulate levoglucosan from burning mukusi, cow dung, mokala, mopane leaves, wanza, and Sub-Saharan African fuel mix are 1090 mg kg^{-1}, 19.7 mg kg^{-1}, 2170 mg kg^{-1}, 178 mg kg^{-1}, 536 mg kg^{-1}, and 758 mg kg^{-1}, respectively. Andreae[7] combined EFs from several sources to create global EF estimates for burning various plant biome groups. The plant biome groups from their study that most closely reflect Sub-Saharan Africa (including Botswana) are the savannah/grassland, tropical forest, and extratropical forest biomes, with levoglucosan EFs reported as 280, 400, and 750 mg kg^{-1}, respectively.[7] These values are close to the levoglucosan EFs for mopane leaves (180 mg kg^{-1}), wanza (540 mg kg^{-1}), and the Sub-Saharan African fuel mix (760 mg kg^{-1}). This is expected since mopane grows in hot dry regions, such as the savannah biome, and wanza grows in warm moist regions with good rainfall, such as the tropical biome.[99]

When comparing the African BB emissions to the BB emissions from wildfires in the western US wildlands (consisting of desert, wetland, plain and shrub grasslands, montane forests, and temperate forests), the EFs for levoglucosan ranged from 0.004 to 100 mg kg^{-1} in the western US wildlands.[100] This is like all the African fuel types examined in the present study, except for mokala which is higher by a factor of ∼2 than this previously reported upper range for western US BBOA. In addition, Hosseini et al.[101] reported EFs for levoglucosan from BB emissions related to the chaparral biome common to southern Europe, North Africa, and the western US ranging from 20−100 mg kg^{-1}. The chaparral-derived EFs for levoglucosan are lower than most of the African fuel emissions examined during this study, and only cow dung had EFs of 20 mg kg^{-1} for levoglucosan that fall within the chaparral range.[102,103]

It should be noted that levoglucosan and possibly some of the other targeted BBOA compounds measured are semi-volatile. Since our OA mass loadings are higher (e.g., 600−1000 $\mu g\ m^{-3}$, which depends on the type of biomass burned) than ambient levels,[104] levoglucosan will partition more readily to the particulate phase during our chamber studies. As a result, our EFs reported for particulate levoglucosan are likely upper bound estimates for what is likely emitted into the atmosphere from burning these fuels. Furthermore, prior studies have shown that particulate levoglucosan can chemically age by heterogeneous reactions with $^{\bullet}OH$ or by gas-phase $^{\bullet}OH$ reactions of levoglucosan that partitions from BBOA particles to the gas phase.[105−107] The lifetime of levoglucosan against heterogeneous $^{\bullet}OH$ oxidation has been estimated to range from weeks at low RH conditions to a couple of days when RH is closer to ambient conditions.[88,105,106,108]

Effect of Photochemical Aging on the Targeted BBOA Marker Compounds. As shown in Table S6, we observed SOA mass growth (in $\mu g\ m^{-3}$) from all fuels burned after UV lights were turned on, which ranged from 26 to 158 $\mu g\ m^{-3}$. Wall loss correction was not applied to our SMPS data to estimate SOA growth, since the filters used for our targeted GC/EI-MS analyses only collected OA from the chamber that was not lost to the walls. Furthermore, we estimated and provide SOA yields (in mg of SOA produced per kg of fuel burned) in Table S6. Since our study was focused on understanding the targeted BBOA species in fresh versus photoaging, we did not attempt to provide SOA mass closure at the molecular level.

Table S7 in the SI shows the presence or absence of the 16 targeted BBOA marker compounds in the photoaged BB emissions generated from the six African fuels examined. Overall, most of the BBOA marker compounds identified in the fresh BB emissions (Table 4) were also present in the photoaged BB emissions from the same fuels (Table S7). However, three of the targeted BBOA compounds, specifically catechol, resorcinol, and coniferyl alcohol, were removed/transformed by photoaging or partitioned back into the gas phase, as BBOA levels lowered during the experiment where they could have reacted with $^{\bullet}OH$. Resorcinol is present in the fresh BBOA emissions from wanza, the Sub-Saharan African fuel mix, and mokala but is absent in the photoaged emissions from burning these same fuels. We observed a similar trend with particulate coniferyl alcohol, which was present in the fresh BBOA emissions from mukusi, Sub-Saharan African fuel mix, and mokala. Coniferyl alcohol, which formed from the pyrolysis of lignin,[109] tends to degrade easily by reaction with $^{\bullet}OH$ forming new particulate products.[110] The reactivity of coniferyl alcohol with $^{\bullet}OH$ likely explains its decrease or disappearance from BBOA after photoaging. Catechol is also absent in the photoaged BBOA emissions from wanza. Prior studies have demonstrated that oxidation of catechol and resorcinol by $^{\bullet}OH$ during photoaging produces multifunctional compounds that can be found in SOA and aged BBOA, including benzenetriol, glyoxylic acid, and maleic acid.[111,112] Pyrogallol, one of the quantified compounds, is a benzenetriol, and it was detected in the photoaged emissions of the Sub-Saharan African fuel mix. Glyoxylic acid was not found in any of the photoaged emissions. There is tentative support for the presence of maleic acid in all of the photoaged emissions, though it is low in abundance.

Differences in the chemical composition of the fresh vs photoaged BB emissions are further displayed in Figures 2−7 and Table S7 in the SI. The figures depict bar graphs, one for each fuel, and the fractional aerosol mass contributions (in %) of each of the targeted BBOA compounds are compared between the fresh vs photoaged BB emissions. To ensure

https://doi.org/10.1021/acsestair.4c00206
ACS EST Air XXXX, XXX, XXX−XXX

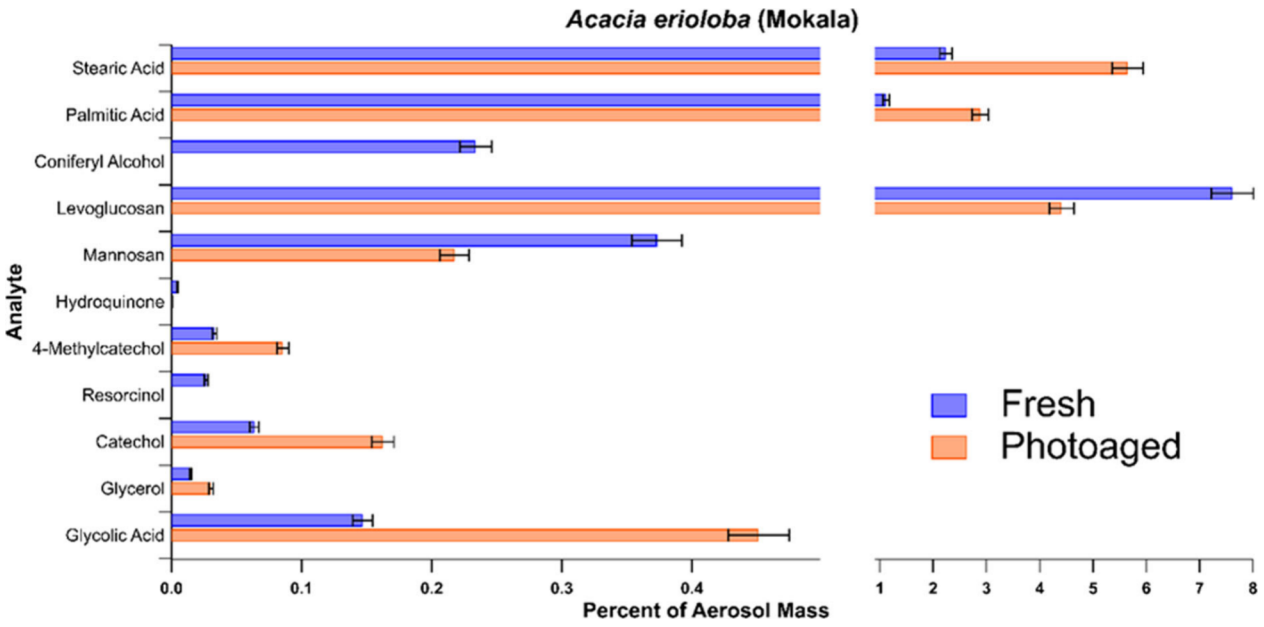

Figure 3. Comparisons of the aerosol mass fractions (in %) of targeted BBOA marker compounds found in both the fresh and photoaged BBOA emissions from mokala. Error bars represent calculated uncertainty in the analytical method.

BBOA compounds with smaller fractional aerosol mass contributions (in %) were not dwarfed by the BBOA compounds with higher aerosol mass fractions, there is a break in each of the *x*-axes (% of total aerosol mass). Table S7 in the SI lists the values associated with Figures 2−7 and compares the fresh vs photoaged BB emissions of the six fuels examined in this study, focusing on the differences between the aerosol mass fractions of the 16 targeted analytes. Since our study only had 3 pairs of replicate burn experiments for 3 fuels (Table S4), there is not enough data to accurately determine the uncertainties associated with burning the same fuel more than once. Therefore, the error bars shown in Figures 2−7 represent only the analytical uncertainties.

In every BBOA sample, except those from mopane leaves and cow dung, the fresh and photoaged aerosol mass fractions of levoglucosan make up the largest percentage of the total aerosol mass (1.0−7.6%). As shown in Figures 3−7, after photoaging, the aerosol mass fraction of levoglucosan decreases in BBOA collected from mopane leaves (1.0% to 0.7%), wanza (2.9% to 1.1%), the Sub-Saharan African fuel mix (3.2% to 2.4%), mukusi (4.7% to 2.0%), and mokala (6.7% to 4.0%); all the percent aerosol masses for levoglucosan are quantifiable. Results from a paired *t*-test of these changes in individual tracers in terms of percent aerosol mass are statistically significant, with a 95% confidence interval. These decreases in levoglucosan aerosol mass fraction in African BBOA with photoaging are consistent with prior studies.[38,73,113] The decrease in levoglucosan could be the result of the formation of new compounds via reactions with •OH radicals. Glucic, formic, and acetic acids can all be formed from the reaction of levoglucosan and •OH radical and are possible photoaging products.[88,114] In cow dung, the levoglucosan aerosol mass fraction change with photoaging is negligible (0.16% to 0.17%) and has a much lower aerosol mass fraction in either fresh or photoaged BBOA emissions compared to the other African biomass fuels (Figure 2). Cow dung is the only fuel examined that is not solely plant matter, and thus, there is significantly less cellulose and hemicellulose readily available to create the aerosol mass fractions of levoglucosan observed from burning the African plant fuels.

Mannosan, a known BBOA isomer of levoglucosan,[115] follows a similar trend to levoglucosan described above (i.e., decreases with photoaging); however, it has a much lower initial aerosol mass fraction. Mannosan is present in BBOA samples derived from mopane leaves, mokala, and the Sub-Saharan African fuel mix. In mopane leaves, mokala, and the Sub-Saharan African fuel mix, mannosan decreases from 0.09% to 0.07%, from 0.37% to 0.22%, and from 0.12% to 0.05%, respectively. These changes were determined to not be statistically significant with a 95% confidence interval when using a one-tailed paired *t*-test of the individual differences.

Coniferyl alcohol in BBOA derived from burning mukusi, wanza, and mokala, the Sub-Saharan African fuel mix decreases in aerosol mass fractions from 1.37% to ND (nondetectable), 1.40% to 0.73%, 0.23% to ND, and 0.40% to ND (all values are quantifiable, and above the LOQ), respectively, after photoaging. The decrease in the percent aerosol mass for coniferyl alcohol was determined to be statistically significant in a 95% confidence interval when using a one-tailed paired *t*-test of the individual differences.

The aerosol mass fraction of catechol appeared to increase after photoaging in all fuels except for negligible changes from mopane leaves (0.12% to 0.09%) and the Sub-Saharan African fuel mix (0.08% to 0%). Catechol also had the lowest initial aerosol mass fractions in these two biomass fuels. The lower initial aerosol mass fraction of catechol in mopane leaves is most likely due to there being less lignin in the leafy portion of the plant since lignin is a structural component for stability in plant stems and woody trunks.[85] The increase in the aerosol mass fractions of catechol upon photoaging in BBOA derived from the other fuels, such as mukusi (0.14% to 0.27%), cow dung (0.16% to 0.26%), mokala (0.06% to 0.16%), and wanza (0.16% to 0.29%), could be due to larger lignin-based structures breaking down due to photochemical mechanisms reactions that form more catechol.[109]

https://doi.org/10.1021/acsestair.4c00206
ACS EST Air XXXX, XXX, XXX−XXX

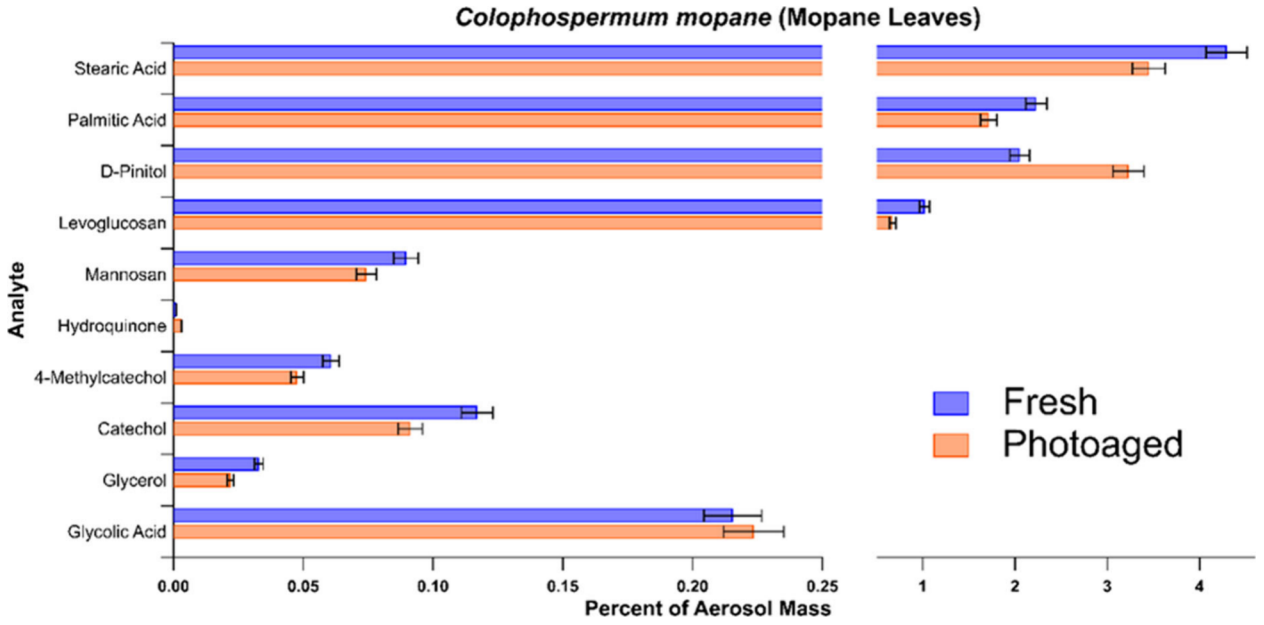

Figure 4. Comparisons of the aerosol mass fractions (in %) of targeted BBOA marker compounds found in both the fresh and photoaged BBOA emissions from mopane leaves. Error bars represent calculated uncertainty in the analytical method.

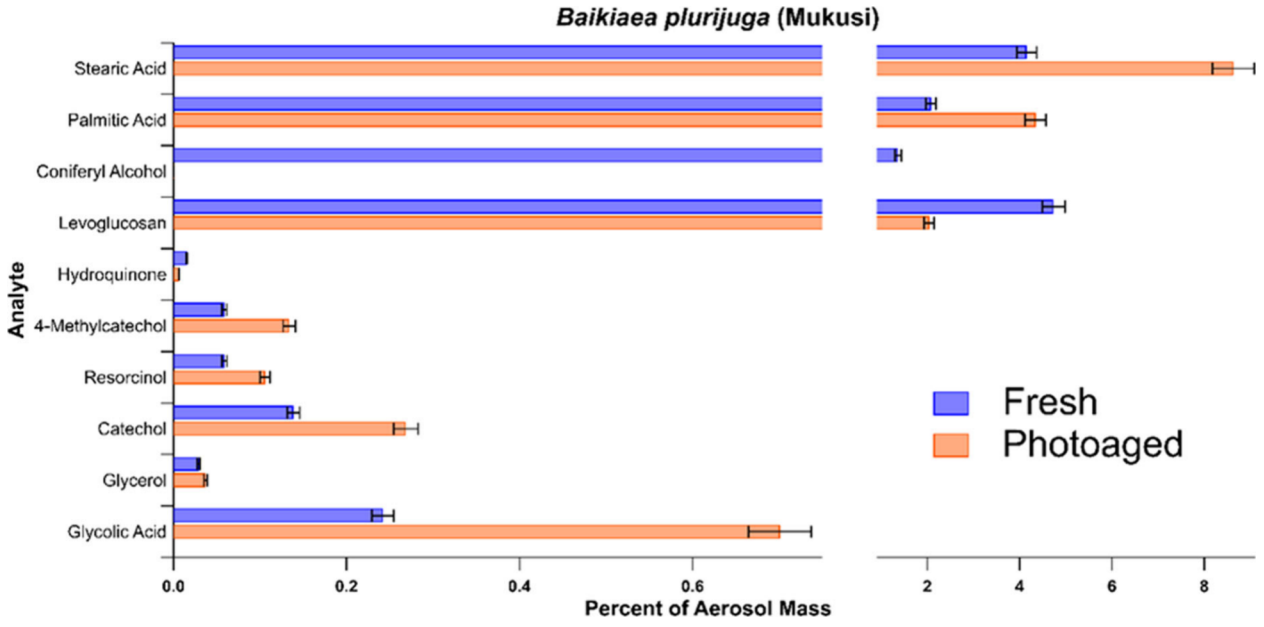

Figure 5. Comparisons of the aerosol mass fractions (in %) of targeted BBOA marker compounds found in both the fresh and photoaged BBOA emissions from mukusi. Error bars represent calculated uncertainty in the analytical method.

Palmitic acid is present in BBOA samples derived from all fresh and photoaged BB emissions. The aerosol mass fractions of palmitic acid tended to increase for mukusi (2.08% to 4.35%), cow dung (3.72% to 4.53%), mokala (1.12% to 2.66%), and wanza (2.50% to 5.34%) after photoaging BB emissions. However, the aerosol mass fractions of palmitic acid were seen to decrease for mopane leaves (2.28% to 1.83%) and the Sub-Saharan African fuel mix (1.53% to 1.06%) after photoaging. The increase in palmitic acid is a result of its low volatility. While other species react away or evaporate after the UV lights are turned on, palmitic acid remains in the aerosol form (this is the same for stearic acid).[116] Our findings are consistent with Sengupta et al.[73] that showed as fatty acid chains varied by Alaskan peat, Moscow peat, Malaysian peat, and eucalyptus after photoaging.

Tentatively Identified BBOA Marker Compounds from Photochemical Aging of Fresh BB Emissions. Table S8 in the SI summarizes the compounds found during the nontargeted GC/EI-MS analysis of the photoaged BBOA and tentatively identifies BBOA marker compounds using the NIST Library associated with the software Qualitative Analysis of MassHunter Acquisition Data 10.0. This table shows the tentative compound names (due to lack of confirmation with authentic compounds), RTs, and the NIST identity probability as well as their presence or absence in each BBOA sample derived from the fuels burned during this study. All of the tentatively identified and listed BBOA marker compounds have

https://doi.org/10.1021/acsestair.4c00206
ACS EST Air XXXX, XXX, XXX−XXX

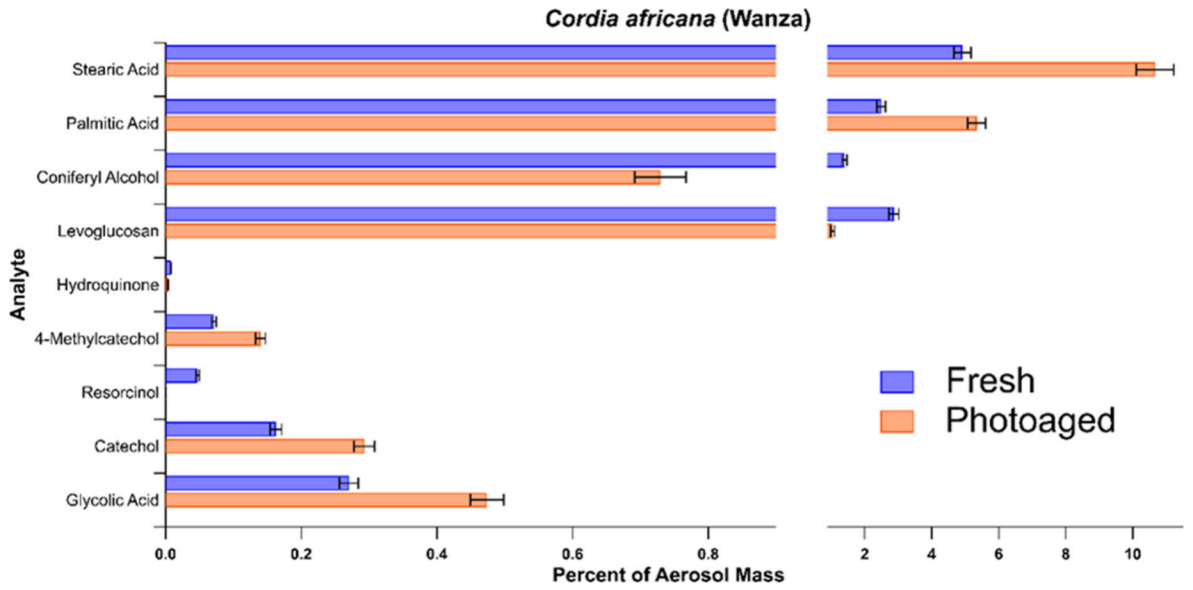

Figure 6. Comparisons of the aerosol mass fractions (in %) of targeted BBOA marker compounds found in both the fresh and photoaged BBOA emissions from wanza. Error bars represent calculated uncertainty in the analytical method.

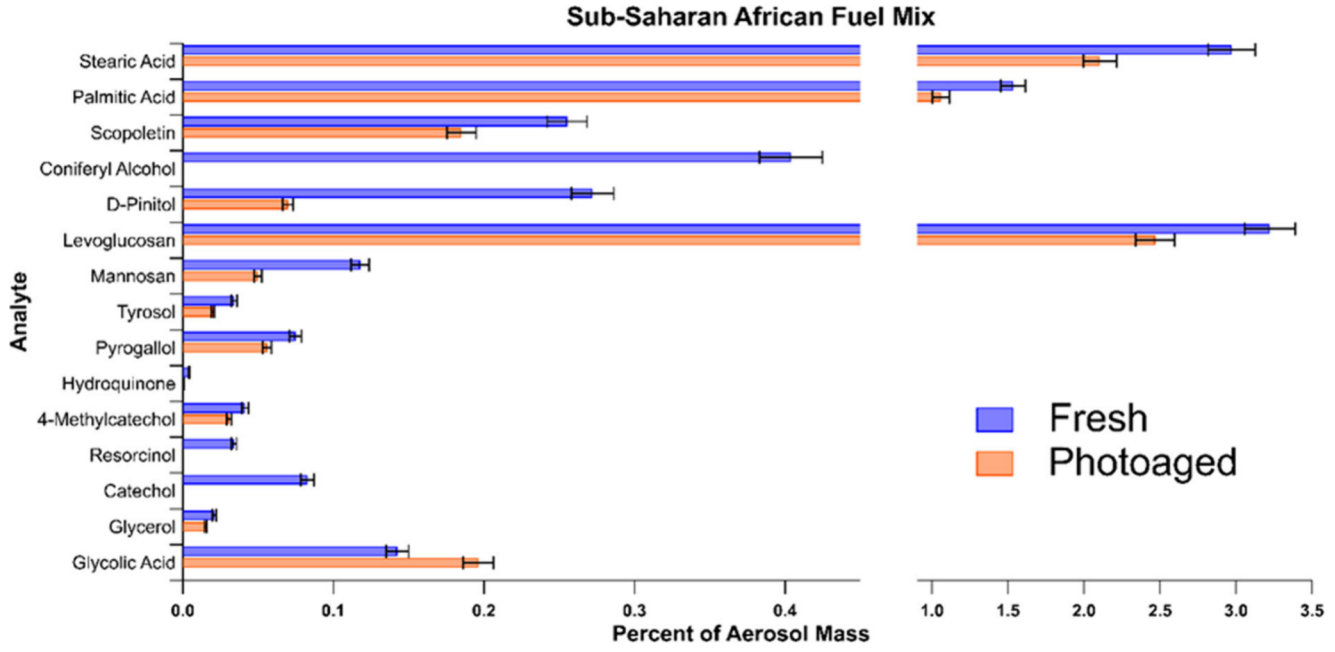

Figure 7. Comparisons of the aerosol mass fractions (in %) of targeted BBOA marker compounds found in both the fresh vs photoaged BBOA emissions from the Sub-Saharan African fuel mix. Error bars represent calculated uncertainty in the analytical method.

a NIST identity probability of at least 56%. The tentatively identified BBOA marker compounds include oxalic, linalool, diethylene glycol, and butanedioic acid. Oxalic acid and butanedioic acids are present in all six fuels.

Diethylene glycol is present only in BBOA collected from wanza and the Sub-Saharan African fuel mix. Linalool is present only in the BBOA collected from mopane leaves, mukusi, mokala, and the Sub-Saharan African fuel mix. Linalool is a known monoterpene released from certain vegetation[117] and has been observed in the gas phase from vegetative emissions.[118] Furthermore, linalool oxidation is known to be an atmospheric source of SOA.[118−120]

Some of the tentatively proposed BBOA marker compounds listed in Table S8 in the SI are present in both the fresh and photoaged BB emissions. Diethylene glycol was present in the fresh BBOA emissions from mukusi, mokala, and the Sub-Saharan African fuel mix while also being present in the photoaged emissions of wanza and the Sub-Saharan African fuel mix. Butanedioic acid is present in all of the fuels in both the fresh and photoaged emissions.

D-Pinitol as a Potential Unique Molecular Tracer for African-Derived BBOA. D-Pinitol is present only in both fresh and photoaged BBOA emissions of mopane leaves and the Sub-Saharan African fuel mix (Figures 4 and 7). The EF of particulate D-pinitol from mopane leaves is 358.0 mg kg^{-1}, which is ∼2 times higher than the EFs of particulate levoglucosan from this same biomass fuel (178.12 mg kg^{-1}, see Table 3). This is unusual because in all other samples,

https://doi.org/10.1021/acsestair.4c00206
ACS EST Air XXXX, XXX, XXX−XXX

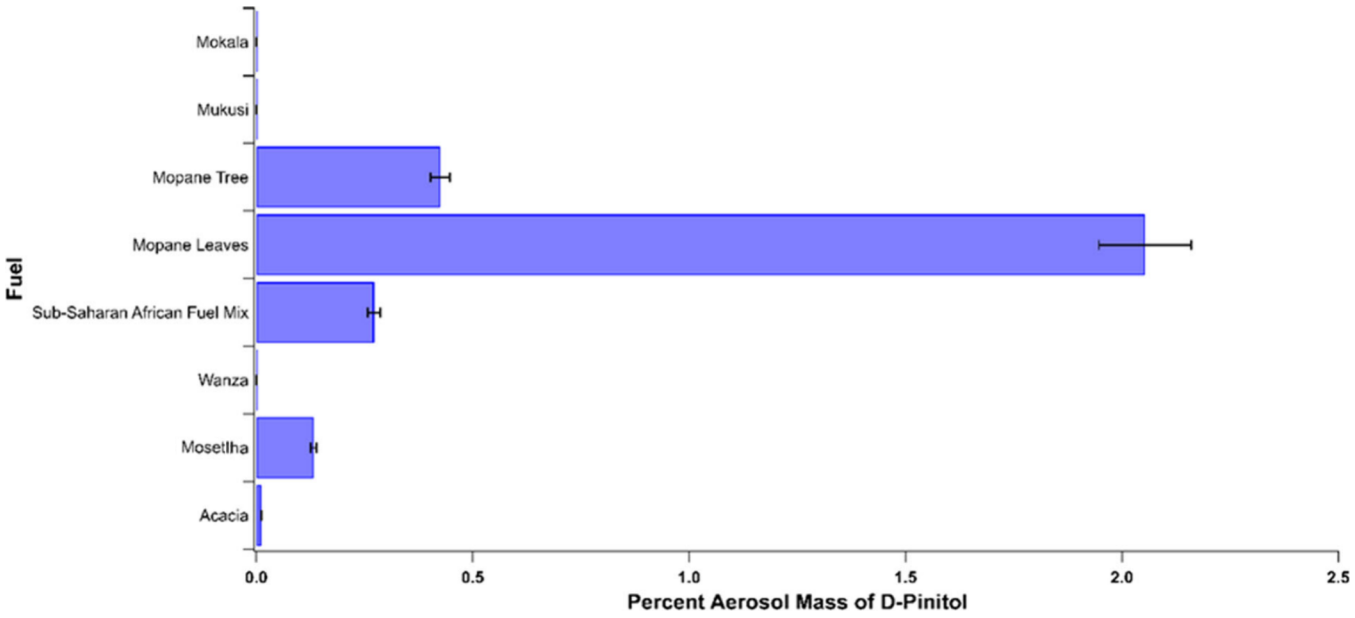

Figure 8. Aerosol mass fractions (in %) of D-pinitol measured from fresh emissions of nine different fuels. Error bars represent calculated uncertainty in the analytical method.

except for cow dung, the EFs of particulate levoglucosan were the largest of the targeted BBOA marker compounds measured during this study. Levoglucosan has been frequently reported in past studies[7,73,77] as having large aerosol mass fractions (16.6−30.9%) and EFs (21−790 mg kg^{-1}). However, upon comparison of the aerosol mass fractions of D-pinitol from the fresh and photoaged BB emissions of mopane leaves, both the fresh and photoaged aerosol mass fractions of D-pinitol were higher than those of levoglucosan and most of the other fresh emissions of the targeted BBOA compounds. D-Pinitol is derived from inositol (natural cyclols and polyols) in plants.[121] There have been several studies on the inositols in BB emissions, and D-pinitol has been previously identified as one of the inositols present; however, D-pinitol has seldom been focused on when it comes to analyzing the concentrations and trends of compounds produced from wildfire BB emissions.[6,77,122]

In a study conducted by Marynowski et al.,[123] D-pinitol was one of three saccharides analyzed to see how concentrations varied over different seasonal weather patterns. D-Pinitol and the other saccharides are directly associated as pollen grain tracers, and it was found that while other pollen grain tracer concentrations depended on blooming season (increasing in the spring and decreasing during the winter), D-pinitol still had a high concentration during the wintertime (when overall pollen concentrations were low). It was this observation that prompted them to conclude that D-pinitol was not only a pollen grain tracer but also a BB tracer.[123] The concentration of D-pinitol would increase during the winter due to the increase in BB emissions produced from home heating. D-Pinitol has been extensively examined by botanical and pharmacological researchers due to its natural ability to regulate insulin.[124−126] It was through these studies that D-pinitol was found to have high concentrations in the Fabaceae or Legume plant family, and plants in the Legume family have been identified as the primary source of natural D-pinitol.[127] A prior study[128] investigated which plants had been used to extract D-pinitol over the past 71 years, and 227 of the 291 extractions were plants in the Fabaceae family.

Mopane leaves (or *Colophospermum mopane*) are a part of the Legume family, and several of the fuels used in the Sub-Saharan African fuel mix examined in our study are also associated with the Fabaceae family. The high concentration of D-pinitol in mopane leaves is explained by its familial origins. In addition, since mopane leaves are specifically the leafy portion of the plant, it has been shown for many legumes that the leaves have the highest D-pinitol concentration compared to other parts of the plant (stems/trunks and roots).[129,130] To confirm that the presence of D-pinitol was not just present in mopane leaves, Figure 8 shows the aerosol mass fractions of D-pinitol measured from the fresh BB emissions of the six fuels, along with its emissions from mopane bark, acacia, and mosetlha. Figure 8 shows that D-pinitol is not just present in the leaves of mopane but also present in the bark of mopane, acacia, and mosetlla. All the fuels that have D-pinitol present in the BBOA samples are part of the Fabaceae family.

Africa is home to a unique plant biomass; however, many of the plant species in Africa belong to only a few plant families.[131] Therefore, the largest percentage of Africa's and Botswana's plant biomass is part of the Fabaceae (legume) family at 12% and 18%, respectively, and the large legume family makeup of Africa's plant biomass is unique to other continents. Both percentages have biomass abundance greater than any other family in these region.[132] The high abundance of legumes in Africa paired with the high natural concentrations of D-pinitol in many of these legumes raises the question if D-pinitol could be used as a BBOA tracer from burning these legumes, and if so, can it also be used as an African specific BBOA molecular tracer due to Africa's biomass makeup.

From the chemical data collected in this study, there is confirmation that D-pinitol has measurable quantities in BBOA samples collected from burning some of the legume fuel species (mopane, acacia, and mosetlha) along with BBOA samples collected from burning the Sub-Saharan African fuel

https://doi.org/10.1021/acsestair.4c00206
ACS EST Air XXXX, XXX, XXX−XXX

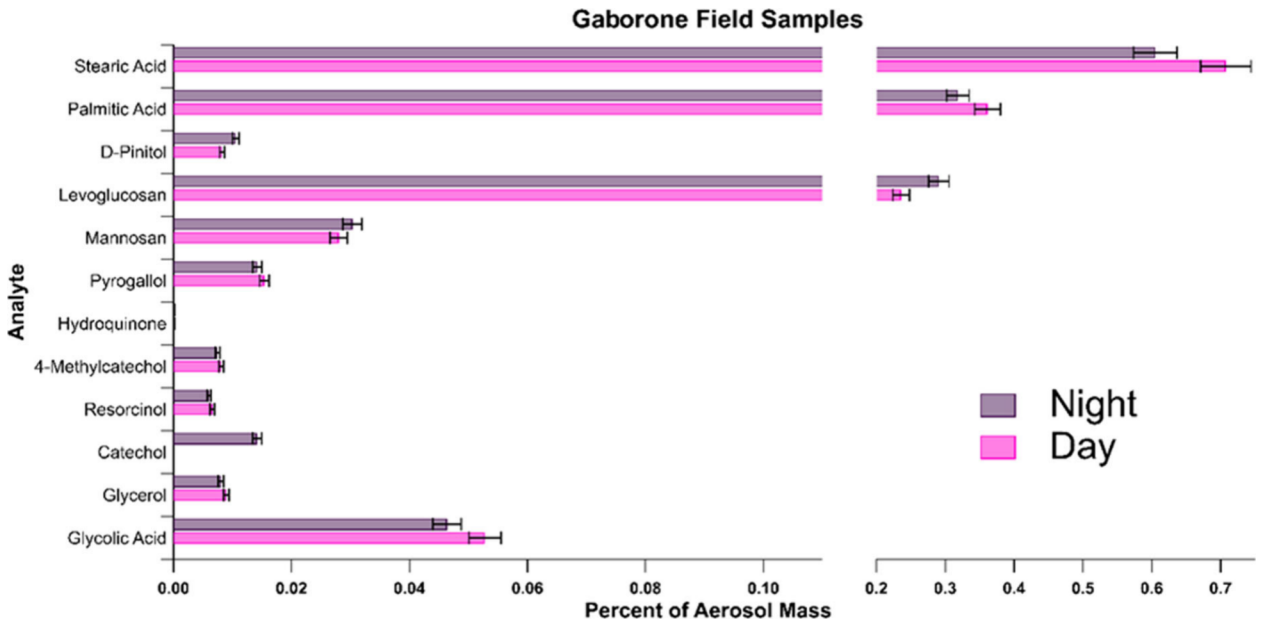

Figure 9. Night vs day ambient aerosol samples were collected from Gaborone, Botswana, during an active wildfire. Error bars represent calculated uncertainty in the analytical method.

mix and in ambient aerosol field samples collected from Botswana (see the subsequent section below). However, there are BBOA samples generated from burning some legume fuels, such as mokala and mukusi, in this study that did not yield particulate D-pinitol. This could be due to the fuels being sourced from the woody portion of the plants and, as a result, they are not being measured from the bark.[129,130] There is also the possibility that D-pinitol might not be present in these legumes, especially since some prior studies have noted that not every legume has high amounts of (or any) D-pinitol even though a large majority of them do.[127,130,133] This study only analyzed a few out of the 1500 legume species that reside in Africa, and the concentrations of D-pinitol in most of these species remain unknown.[131] To summarize, as noted above in the prior studies discussed, D-pinitol has naturally high concentrations in most legumes, and it could be identified in BBOA samples collected from wildfire emissions occurring in Botswana. This suggests that D-pinitol could also be measured in BBOA samples collected from wildfire emissions occurring from other African countries because of the high density and abundance of Fabaceae plants on the continent. D-Pinitol should be further explored as a possible BBOA tracer for burning legumes from other African countries. D-Pinitol in tandem with other possibly unique BBOA tracers for legumes and African BB emissions may be unique enough and in sufficiently high concentrations to potentially tie the analytes back to African biomass sources. Future work should also examine how D-pinitol transforms during atmospheric chemical aging due to its likely presence in ambient $PM_{2.5}$ samples collected from Africa, especially since similar molecules, such as levoglucosan, have been shown to undergo these transformations.[73,113,134]

Atmospheric Implications: Comparison of Laboratory-Identified BBOA Marker Compounds versus Ambient Samples Collected from Botswana. Figure 9 shows the targeted BBOA marker compounds identified in aerosol samples collected during one of the ambient aerosol sampling periods at the Gaborone, Botswana, ground site. The aerosol sampling was conducted for a 12-h period during the night, and then the sampling continued into the next day for another 12-h period. The sample was chosen because of the heavy use of solid fuels for heating and cooking during the time of both the night and day sampling. Figure 9 compares the nighttime and daytime measured aerosol mass fractions (in %) of the 16 targeted BBOA compounds. The fuel that reflects the ambient aerosol emissions collected from the field the best is the Sub-Saharan African fuel mix, which has a mixture of wanza, mukusi, mokala, mopane leaves, cow dung, savannah grass, acacia, mosetlha, wild olive, and eucalyptus.

The Sub-Saharan African fuel mix has every targeted BBOA marker compound present except for hydroxytyrosol (Tables 2 and S4). In the aerosol samples collected from Gaborone, coniferyl alcohol, hydroxytyrosol, tyrosol, and scopoletin are not present (Figure 9). As observed from our studies with the Sub-Saharan African fuel mix, levoglucosan, mannosan, and catechol all decrease in the Gaborone aerosol samples as these compounds are exposed to light during the daytime (Figure 9). This decrease could be due to the compounds being used up in atmospheric photochemical reactions or due to the dilution that can be caused by the rising of the planetary boundary layer (PBL) during the daytime. If the decrease in percent aerosol mass of the compounds is solely caused by the rise of the PBL, then all of the compounds analyzed would decrease in percent aerosol mass. This is not the case for the Gaborone data as palmitic acid, stearic acid, glycolic acid, glycerol, 4-methylcatechol, and pyrogallol all increase in percent aerosol mass during the daytime (Figure 9), supporting that the decrease in some of the compounds could be due (at least in part) to atmospheric photochemical reactions using up the compounds. The increase observed in palmitic and stearic acid could be the result of cooking activities producing the acids during the daytime.[116] Levoglucosan in the Gaborone aerosol samples has the third highest aerosol mass fraction, which is like the Sub-Saharan African fuel mix (Figure 7). Catechol in the Sub-Saharan African fuel mix is present in the fresh emissions and then is almost completely removed after photoaging (Figure

https://doi.org/10.1021/acsestair.4c00206
ACS EST Air XXXX, XXX, XXX−XXX

7). This trend is also observed in the Gaborone aerosol samples, as catechol is present in the nighttime aerosol sample but is mostly removed from the subsequent daytime aerosol sample. The similarities between the trends observed between the laboratory chamber-derived and ambient aerosol samples are encouraging, but a more intensive field study should be conducted in this region to confirm our initial findings.

D-Pinitol is present in BBOA generated from the laboratory burns of the Sub-Saharan African fuel mix, emphasizing that it will be present in a mixture of fuels and not just in an individual fuel. The ambient aerosol samples collected from Gaborone, Botswana, also have D-pinitol present, highlighting that D-pinitol is not just limited to laboratory emissions and is likely a product of real-world BB events. The presence of D-pinitol in ambient aerosol collected from Botswana coincides with the fact that a majority of African and Botswanan biomass is a part of the Fabaceae family, further emphasizing the possibility of D-pinitol as a unique component of African BBOA emissions or emissions from legumes that could potentially be used in future source apportionment studies.

D-Pinitol was identified as having high aerosol mass concentrations (up to 3.23% of total aerosol mass) and EFs (358 mg kg^{-1}) in the Fabaceae (legume) family, and a majority of African plant biomass are legumes.[131] Due to the presence of D-pinitol in the laboratory-generated BBOA samples from mopane leaves and the Sub-Saharan African fuel mix, as well as in the ambient aerosol samples collected from Gaborone, Botswana, our findings suggest that D-pinitol should be further explored as a possible unique tracer for African- or Legume-sourced BBOA emissions.

In this study, fresh and photoaged BBOA from burning five individual African-specific biomass fuels and one African-specific biomass fuel mix was generated in a smog chamber facility and subsequently analyzed by using GC/EI-MS. Our investigation aimed to identify the presence or absence of 16 target BBOA marker compounds from both the fresh and photoaged emissions, calculate EFs for these target BBOA compounds from the fresh emissions, and determine aerosol mass fraction changes (if any) of these BBOA marker compounds after photoaging. This study also aimed to compare laboratory smog-chamber-generated BBOA samples to field samples collected from Botswana in order to identify if any unique tracers could be used to track African BB emissions. The general trends in the percent aerosol mass fractions of the targeted BBOA maker compounds, such as levoglucosan, mannosan, and palmitic acid, were consistent with prior studies on photoaged aerosols.[64,135] In addition, the presence/absence of many of the targeted BBOA marker compounds from burning Ethiopian cow dung and mopane leaves coincided with the botanical and biological background of the fuels not being the woody portion of the plant (in the case of the mopane leaves) and not being plant matter (in the case of dung).

The results from our study provide an important step forward in exploring more African-specific BBOA compounds in wildfire emissions but also start to examine the crucial relationship between the botanical makeup of plants and the emissions produced when vegetation burns. All in all, there are some limitations to the study. Concentrations in the chamber may be similar to near-source concentrations but do not reflect ambient atmospheric conditions; for example, gas-particle partitioning changes with dilution in the atmosphere, which is a process that is not simulated in the chamber. Chamber experiments were conducted at constant humidity and temperature, which allowed for better analysis of emissions in different fuels but did not explore the effects on emissions due to different atmospheric conditions. In addition, while our EF calculations correct for dilution and wall loss of PM during experiments, they do not account for the potential for differential wall loss of gaseous species, which might affect partitioning and thus species-specific EFs. Even though the chamber experiments can never perfectly replicate the atmosphere, they do provide insight into African BB emissions and atmospheric processing. Further investigation of African-specific BBOA emissions is warranted to draw further connections between the botany of plant biomass and BBOA emissions, which could further aid in the creation of more accurate and effective models. Understanding BBOA emissions from a continent that makes up a large percentage of global BB carbon emissions but has been left out of many research endeavors is needed to improve aerosol-climate models.

■ ASSOCIATED CONTENT

Supporting Information

The Supporting Information is available free of charge at https://pubs.acs.org/doi/10.1021/acsestair.4c00206.

Additional information including details of replicate chamber experiments (Section S1); generation of GC/EI-MS calibration curves and their application for calculating aerosol mass fractions of BBOA constituents (Section S2); GC/EI-MS analysis of filters collected from chamber background, solvent blanks, and filter blanks (Section S3); GC/EI-MS analysis of individual standards versus standards in a mixture (Section S4); determination of reconstitution volumes of derivatizing reagents for GC/EI-MS analysis (Section S5); reproducibility testing for GC/EI-MS (Section S6); filter extraction efficiencies and recoveries of targeted BBOA constituents (Section S7); table with unique GC/EI-MS fragment ions used for each standard (Table S1); table with LODs/LOQs for targeted BBOA compounds (Table S2); table of details for standard stock solutions (Table S3); % aerosol mass of BBOA tracer compounds from the fresh and photoaged emissions of replicate experiments for mokala, mopane, and mukusi (Table S4); table of identified BBOA marker compounds in photoaged BB emissions confirmed by authentic standards (Table S5); table summarizing SOA mass concentrations (and yields) produced from turning UV lights on after sampling fresh (dark) BB emissions (Table S6); table of aerosol mass fractions of the 16 targeted BBOA marker compounds in fresh vs photoaged BBOA emissions from each fuel (Table S7); tentatively identified BBOA marker compounds in photoaged BB emissions (Table S8); table of % recovery of target BBOA compounds during filter sample extraction and workup (Table S9); GC/EI-MS EICs of lactic acid, levoglucosan, D-pinitol, and stearic acid in fresh BBOA samples versus chamber blanks (backgrounds) (Figure S1) (PDF)

■ AUTHOR INFORMATION

Corresponding Authors

Solomon Bililign − *Department of Physics, College of Science and Technology, North Carolina Agricultural and Technical*

https://doi.org/10.1021/acsestair.4c00206
ACS EST Air XXXX, XXX, XXX−XXX

State University, Greensboro, North Carolina 27411, United States; Email: bililign@ncat.edu

Jason D. Surratt − *Department of Environmental Sciences and Engineering, Gillings School of Global Public Health, University of North Carolina at Chapel Hill, Chapel Hill, North Carolina 27599, United States; Department of Chemistry, College of Arts and Sciences, University of North Carolina at Chapel Hill, Chapel Hill, North Carolina 27599, United States;* orcid.org/0000-0002-6833-1450; Email: surratt@unc.edu

Authors

Adrienne M. Lambert − *Department of Environmental Sciences and Engineering, Gillings School of Global Public Health, University of North Carolina at Chapel Hill, Chapel Hill, North Carolina 27599, United States*

Cade M. Christensen − *Department of Chemistry, College of Arts and Sciences, University of North Carolina at Chapel Hill, Chapel Hill, North Carolina 27599, United States*

Megan M. McRee − *Applied Sciences and Technology Program, North Carolina Agricultural and Technical State University, Greensboro, North Carolina 27411, United States;* orcid.org/0009-0001-8946-2329

Vaios Moschos − *Department of Environmental Sciences and Engineering, Gillings School of Global Public Health, University of North Carolina at Chapel Hill, Chapel Hill, North Carolina 27599, United States; Department of Physics, College of Science and Technology, North Carolina Agricultural and Technical State University, Greensboro, North Carolina 27411, United States;* orcid.org/0000-0002-6251-4117

Markiesha H. James − *Department of Chemistry, North Carolina Agricultural and Technical State University, Greensboro, North Carolina 27411, United States*

Janica N. D. Gordon − *Applied Sciences and Technology Program, North Carolina Agricultural and Technical State University, Greensboro, North Carolina 27411, United States*

Haley M. Royer − *Department of Environmental Sciences and Engineering, Gillings School of Global Public Health, University of North Carolina at Chapel Hill, Chapel Hill, North Carolina 27599, United States*

Marc N. Fiddler − *Department of Chemistry, North Carolina Agricultural and Technical State University, Greensboro, North Carolina 27411, United States;* orcid.org/0000-0003-3733-5800

Barbara J. Turpin − *Department of Environmental Sciences and Engineering, Gillings School of Global Public Health, University of North Carolina at Chapel Hill, Chapel Hill, North Carolina 27599, United States;* orcid.org/0000-0003-4513-4187

Complete contact information is available at: https://pubs.acs.org/10.1021/acsestair.4c00206

Notes

The authors declare no competing financial interest.

■ ACKNOWLEDGMENTS

This research was primarily supported by the United States (US) National Science Foundation (NSF) through the Atmospheric & Geospace Sciences (AGS) Division grant # 2100708. V.M. acknowledges support from the Swiss National Science Foundation (SNSF) under the Postdoc Mobility Fellowship grant P500PN_210745. Ambient aerosol collection was funded by the US NSF Office of International Science & Engineering (OISE) Division grant # 1559308. We thank Gizaw Mengistu Tsidu (BIUST) for providing biomass fuel samples from Botswana and his support during the BIUST field campaign and Christina Isaxon (Lund University) for providing the cow-dung fuel sample from Ethiopia. We thank Kip Carrico and Mercy Ikes at New Mexico Tech University for the moisture content analysis of all fuels examined in our study.

■ ABBREVIATIONS

BB, Biomass burning; BBOA, Biomass burning organic aerosols; BrC, Brown carbon; BSTFA, N,O-Bis(trimethylsilyl)-trifluoroacetamide; EF, Emission factor; EIC, Extracted ion chromatogram; GC/EI-MS, Gas chromatography interfaced to an electron ionization mass spectrometer; LCMS, Liquid chromatography mass spectrometry; NIST, National Institute of Standards and Technology; PBL, Planetary Boundary Layer; PM, Particulate matter; $PM_{2.5}$, Particulate matter under 2.5 μm in diameter; RH, Relative humidity; RT, Retention time; SMPS, Scanning mobility particle sizer; SOA, Secondary organic aerosol; TIC, Total ion chromatogram; TMS, Trimethylsilyl; μ, micro

■ REFERENCES

(1) Barker, P. A.; Allen, G.; Gallagher, M.; Pitt, J. R.; Fisher, R. E.; Bannan, T.; Nisbet, E. G.; Bauguitte, S. J. B.; Pasternak, D.; Cliff, S.; et al. Airborne measurements of fire emission factors for African biomass burning sampled during the MOYA campaign. *Atmos. Chem. Phys.* **2020**, *20* (23), 15443−15459.

(2) Montzka, S. A.; Dlugokencky, E. J.; Butler, J. H. Non-CO2 greenhouse gases and climate change. *Nature* **2011**, *476* (7358), 43−50.

(3) IPCC, 2013: *Climate Change 2013: The Physical Science Basis. Contribution of Working Group I to the Fifth Assessment Report of the Intergovernmental Panel on Climate Change*; Stocker, T. F., Qin, D., Plattner, G.-K., Tignor, M., Allen, S. K., Boschung, J., Nauels, A., Xia, Y., Bex, V., Midgley, P. M., Eds.; Cambridge University Press, Cambridge, United Kingdom and New York, NY, USA, 1535pp.

(4) Lignell, H.; Hinks, M. L.; Nizkorodov, S. A. Exploring matrix effects on photochemistry of organic aerosols. *Proc. Natl. Acad. Sci. U. S. A.* **2014**, *111* (38), 13780−13785.

(5) Jones, M. W.; Abatzoglou, J. T.; Veraverbeke, S.; Andela, N.; Lasslop, G.; Forkel, M.; Smith, A. J. P.; Burton, C.; Betts, R. A.; van der Werf, G. R.; et al. Global and Regional Trends and Drivers of Fire Under Climate Change. *Reviews of Geophysics* **2022**, *60* (3), No. e2020RG000726.

(6) Xu, R.; Yu, P.; Abramson, M. J.; Johnston, F. H.; Samet, J. M.; Bell, M. L.; Haines, A.; Ebi, K. L.; Li, S.; Guo, Y. Wildfires, Global Climate Change, and Human Health. *New England Journal of Medicine* **2020**, *383* (22), 2173−2181.

(7) Andreae, M. O. Emission of trace gases and aerosols from biomass burning - an updated assessment. *Atmos. Chem. Phys.* **2019**, *19* (13), 8523−8546.

(8) Tian, H.; Lu, C.; Ciais, P.; Michalak, A. M.; Canadell, J. G.; Saikawa, E.; Huntzinger, D. N.; Gurney, K. R.; Sitch, S.; Zhang, B.; et al. The terrestrial biosphere as a net source of greenhouse gases to the atmosphere. *Nature* **2016**, *531* (7593), 225−228.

(9) Andreae, M. O.; Merlet, P. Emission of Trace Gases and Aerosols from Biomass Burning. *Global Biogeochem. Cycles* **2001**, *15* (4), 955.

(10) Park, R. J.; Jacob, D. J.; Logan, J. A. Fire and biofuel contributions to annual mean aerosol mass concentrations in the United States. *Atmos. Environ.* **2007**, *41* (35), 7389−7400.

(11) Pardo, M.; Li, C.; He, Q.; Levin-Zaidman, S.; Tsoory, M.; Yu, Q.; Wang, X.; Rudich, Y. Mechanisms of lung toxicity induced by

biomass burning aerosols. *Particle and Fibre Toxicology* **2020**, *17* (1), 4.
(12) Lelieveld, J.; Evans, J. S.; Fnais, M.; Giannadaki, D.; Pozzer, A. The contribution of outdoor air pollution sources to premature mortality on a global scale. *Nature* **2015**, *525* (7569), 367−371.
(13) Black, C.; Tesfaigzi, Y.; Bassein, J. A.; Miller, L. A. Wildfire smoke exposure and human health: Significant gaps in research for a growing public health issue. *Environmental Toxicology and Pharmacology* **2017**, *55*, 186−195.
(14) Basith, S.; Manavalan, B.; Shin, T. H.; Park, C. B.; Lee, W.-S.; Kim, J.; Lee, G. The Impact of Fine Particulate Matter 2.5 on the Cardiovascular System: A Review of the Invisible Killer. *Nanomaterials* **2022**, *12* (15), 2656.
(15) U.S. EPA, Particulate Matter (PM Basics), 2024. https://www.epa.gov/pm-pollution/particulate-matter-pm-basics.
(16) Johnston, F. H.; Henderson, S. B.; Chen, Y.; Randerson, J. T.; Marlier, M.; Defries, R. S.; Kinney, P.; Bowman, D. M. J. S.; Brauer, M. Estimated Global Mortality Attributable to Smoke from Landscape Fires. *Environ. Health Perspect.* **2012**, *120* (5), 695.
(17) Gordon, J. N. D.; Bilsback, K. R.; Fiddler, M. N.; Pokhrel, R. P.; Fischer, E. V.; Pierce, J. R.; Bililign, S. The Effects of Trash, Residential Biofuel, and Open Biomass Burning Emissions on Local and Transported PM2.5 and Its Attributed Mortality in Africa. *GeoHealth* **2023**, *7* (2), No. e2022GH000673.
(18) Chen, S.-L.; Chang, S.-W.; Chen, Y.-J.; Chen, H.-L. Possible warming effect of fine particulate matter in the atmosphere. *Communications Earth & Environment* **2021**, *2* (1), 208.
(19) Kanakidou, M.; Seinfeld, J. H.; Pandis, S. N.; Barnes, I.; Dentener, F. J.; Facchini, M. C.; Van Dingenen, R.; Ervens, B.; Nenes, A.; Nielsen, C. J.; et al. Organic aerosol and global climate modelling: a review. *Atmos. Chem. Phys.* **2005**, *5* (4), 1053−1123.
(20) IPCC, 2001: *Climate Change 2001: The Scientific Basis. Contribution of Working Group I to the Third Assessment Report of the Intergovernmental Panel on Climate Change*; Houghton, J. T., Ding, Y., Griggs, D. J., Noguer, M., Linden, P. J. van der, Dai, X., Maskell, K., Johnson, C.A., Eds.; Cambridge University Press, Cambridge, United Kingdom and New York, NY, USA, 881pp.
(21) Liang, L.; Engling, G.; Liu, C.; Xu, W.; Liu, X.; Cheng, Y.; Du, Z.; Zhang, G.; Sun, J.; Zhang, X. Measurement report: Chemical characteristics of PM2.5 during typical biomass burning season at an agricultural site of the North China Plain. *Atmos. Chem. Phys.* **2021**, *21* (4), 3181−3192.
(22) Khan, J. Z.; Sun, L.; Tian, Y.; Shi, G.; Feng, Y. Chemical characterization and source apportionment of PM1 and PM2.5 in Tianjin, China: Impacts of biomass burning and primary biogenic sources. *Journal of Environmental Sciences* **2021**, *99*, 196−209.
(23) Zhang, X.; Xu, J.; Kang, S.; Liu, Y.; Zhang, Q. Chemical characterization of long-range transport biomass burning emissions to the Himalayas: insights from high-resolution aerosol mass spectrometry. *Atmos. Chem. Phys.* **2018**, *18* (7), 4617−4638.
(24) Khamkaew, C.; Chantara, S.; Janta, R.; Pani, S. K.; Prapamontol, T.; Kawichai, S.; Wiriya, W.; Lin, N.-H. Investigation of Biomass Burning Chemical Components over Northern Southeast Asia during 7-SEAS/BASELInE 2014 Campaign. *Aerosol and Air Quality Research* **2016**, *16* (11), 2655−2670.
(25) Diapouli, E.; Popovicheva, O.; Kistler, M.; Vratolis, S.; Persiantseva, N.; Timofeev, M.; Kasper-Giebl, A.; Eleftheriadis, K. Physicochemical characterization of aged biomass burning aerosol after long-range transport to Greece from large scale wildfires in Russia and surrounding regions, Summer 2010. *Atmos. Environ.* **2014**, *96*, 393−404.
(26) Saarikoski, S.; Sillanpää, M.; Sofiev, M.; Timonen, H.; Saarnio, K.; Teinilä, K.; Karppinen, A.; Kukkonen, J.; Hillamo, R. Chemical composition of aerosols during a major biomass burning episode over northern Europe in spring 2006: Experimental and modelling assessments. *Atmos. Environ.* **2007**, *41* (17), 3577−3589.
(27) Lanz, V. A.; Prévôt, A. S. H.; Alfarra, M. R.; Weimer, S.; Mohr, C.; DeCarlo, P. F.; Gianini, M. F. D.; Hueglin, C.; Schneider, J.; Favez, O.; et al. Characterization of aerosol chemical composition with aerosol mass spectrometry in Central Europe: an overview. *Atmos. Chem. Phys.* **2010**, *10* (21), 10453−10471.
(28) Zhou, S.; Collier, S.; Jaffe, D. A.; Briggs, N. L.; Hee, J.; Sedlacek, A. J.; Kleinman, L.; Onasch, T. B.; Zhang, Q. Regional Influence of Wildfires on Aerosol Chemistry in the Western US and Insights into Atmospheric Aging of Biomass Burning Organic Aerosol. *Atmos. Chem. Phys.* **2017**, *17* (3), 2477.
(29) Silva, P. J.; Liu, D.-Y.; Noble, C. A.; Prather, K. A. Size and Chemical Characterization of Individual Particles Resulting from Biomass Burning of Local Southern California Species. *Environ. Sci. Technol.* **1999**, *33* (18), 3068−3076.
(30) Liang, Y.; Jen, C. N.; Weber, R. J.; Misztal, P. K.; Goldstein, A. H. Chemical composition of PM2.5 in October 2017 Northern California wildfire plumes. *Atmos. Chem. Phys.* **2021**, *21* (7), 5719−5737.
(31) Hyer, E.; Wang, J.; Arellano, A. Biomass Burning: Observations, Modeling, and Data Assimilation. *Bulletin of the American Meteorological Society* **2012**, *93* (1), ES10−ES14.
(32) van der Werf, G. R.; Randerson, J. T.; Giglio, L.; Collatz, G. J.; Mu, M.; Kasibhatla, P. S.; Morton, D. C.; DeFries, R. S.; Jin, Y.; van Leeuwen, T. T. Global fire emissions and the contribution of deforestation, savanna, forest, agricultural, and peat fires (1997−2009). *Atmos. Chem. Phys.* **2010**, *10* (23), 11707−11735.
(33) Ichoku, C.; Ellison, L. T.; Willmot, K. E.; Matsui, T.; Dezfuli, A. K.; Gatebe, C. K.; Wang, J.; Wilcox, E. M.; Lee, J.; Adegoke, J.; et al. Biomass burning, land-cover change, and the hydrological cycle in Northern sub-Saharan Africa. *Environmental Research Letters* **2016**, *11* (9), 095005.
(34) Jolly, W. M.; Cochrane, M. A.; Freeborn, P. H.; Holden, Z. A.; Brown, T. J.; Williamson, G. J.; Bowman, D. M. J. S. Climate-induced variations in global wildfire danger from 1979 to 2013. *Nat. Commun.* **2015**, *6* (1), 7537.
(35) Maabong, K. E.; Kgakgamatso, M. Wildfires in Botswana and Their Frequency of Occurrence. *Atmospheric and Climate Sciences* **2021**, *11* (4), 689−696.
(36) Smith, D. M.; Fiddler, M. N.; Sexton, K. G.; Bililign, S. Construction and Characterization of an Indoor Smog Chamber for Measuring the Optical and Physicochemical Properties of Aging Biomass Burning Aerosols. *Aerosol and Air Quality Research* **2019**, *19* (3), 467−483.
(37) Kamens, R. M.; Rives, G. D.; Perry, J. M.; Bell, D. A.; Paylo, R. F.; Goodman, R. G.; Claxton, L. D. Mutagenic changes in dilute wood smoke as it ages and reacts with ozone and nitrogen dioxide. An outdoor chamber study. *Environ. Sci. Technol.* **1984**, *18* (7), 523−530.
(38) Hennigan, C. J.; Miracolo, M. A.; Engelhart, G. J.; May, A. A.; Presto, A. A.; Lee, T.; Sullivan, A. P.; McMeeking, G. R.; Coe, H.; Wold, C. E.; et al. Chemical and Physical Transformations of Organic Aerosol from the Photo-Oxidation of Open Biomass Burning Emissions in an Environmental Chamber. *Atmos. Chem. Phys.* **2011**, *11* (15), 7669.
(39) Liu-Kang, C.; Gallimore, P. J.; Liu, T.; Abbatt, J. P. D. Photoreaction of biomass burning brown carbon aerosol particles. *Environmental Science: Atmospheres* **2022**, *2* (2), 270−278.
(40) Schnitzler, E. G.; Liu, T.; Hems, R. F.; Abbatt, J. P. D. Emerging investigator series: heterogeneous OH oxidation of primary brown carbon aerosol: effects of relative humidity and volatility. *Environmental Science: Processes & Impacts* **2020**, *22* (11), 2162−2171.
(41) Browne, E. C.; Zhang, X.; Franklin, J. P.; Ridley, K. J.; Kirchstetter, T. W.; Wilson, K. R.; Cappa, C. D.; Kroll, J. H. Effect of heterogeneous oxidative aging on light absorption by biomass burning organic aerosol. *Aerosol Sci. Technol.* **2019**, *53* (6), 663−674.
(42) Lim, C. Y.; Hagan, D. H.; Coggon, M. M.; Koss, A. R.; Sekimoto, K.; de Gouw, J.; Warneke, C.; Cappa, C. D.; Kroll, J. H. Secondary organic aerosol formation from the laboratory oxidation of biomass burning emissions. *Atmos. Chem. Phys.* **2019**, *19* (19), 12797−12809.
(43) Akherati, A.; He, Y.; Coggon, M. M.; Koss, A. R.; Hodshire, A. L.; Sekimoto, K.; Warneke, C.; de Gouw, J.; Yee, L.; Seinfeld, J. H.; et al. Oxygenated Aromatic Compounds are Important Precursors of

https://doi.org/10.1021/acsestair.4c00206
ACS EST Air XXXX, XXX, XXX−XXX

Secondary Organic Aerosol in Biomass-Burning Emissions. *Environ. Sci. Technol.* **2020**, *54* (14), 8568−8579.
(44) Ortega, A. M.; Day, D. A.; Cubison, M. J.; Brune, W. H.; Bon, D.; Gouw, J. A.; Jimenez, J. L. Secondary Organic Aerosol Formation and Primary Organic Aerosol Oxidation from Biomass-Burning Smoke in a Flow Reactor during FLAME-3. *Atmos. Chem. Phys.* **2013**, *13* (22), 11551.
(45) Arangio, A. M.; Slade, J. H.; Berkemeier, T.; Pöschl, U.; Knopf, D. A.; Shiraiwa, M. Multiphase Chemical Kinetics of OH Radical Uptake by Molecular Organic Markers of Biomass Burning Aerosols: Humidity and Temperature Dependence, Surface Reaction, and Bulk Diffusion. *J. Phys. Chem. A* **2015**, *119* (19), 4533−4544.
(46) Shen, X.; Zhao, Y.; Chen, Z.; Huang, D. Heterogeneous reactions of volatile organic compounds in the atmosphere. *Atmos. Environ.* **2013**, *68*, 297−314.
(47) Gilardoni, S.; Massoli, P.; Paglione, M.; Giulianelli, L.; Carbone, C.; Rinaldi, M.; Decesari, S.; Sandrini, S.; Costabile, F.; Gobbi, G. P.; et al. Direct observation of aqueous secondary organic aerosol from biomass-burning emissions. *Proc. Natl. Acad. Sci. U. S. A.* **2016**, *113* (36), 10013−10018.
(48) Wang, Q.; Wang, S.; Cheng, Y. Y.; Chen, H.; Zhang, Z.; Li, J.; Gu, D.; Wang, Z.; Yu, J. Z. Chemical evolution of secondary organic aerosol tracers during high-PM2.5 episodes at a suburban site in Hong Kong over 4 months of continuous measurement. *Atmos. Chem. Phys.* **2022**, *22* (17), 11239−11253.
(49) Offer, S.; Hartner, E.; Bucchianico, S. D.; Bisig, C.; Bauer, S.; Pantzke, J.; Zimmermann, E. J.; Cao, X.; Binder, S.; Kuhn, E.; et al. Effect of Atmospheric Aging on Soot Particle Toxicity in Lung Cell Models at the Air-Liquid Interface: Differential Toxicological Impacts of Biogenic and Anthropogenic Secondary Organic Aerosols (SOAs). *Environ. Health Perspect.* **2022**, *130* (2), 027003.
(50) Wong, J. P. S.; Tsagkaraki, M.; Tsiodra, I.; Mihalopoulos, N.; Violaki, K.; Kanakidou, M.; Sciare, J.; Nenes, A.; Weber, R. J. Atmospheric evolution of molecular-weight-separated brown carbon from biomass burning. *Atmos. Chem. Phys.* **2019**, *19* (11), 7319−7334.
(51) Watts, A. C.; Kobziar, L. N. Smoldering Combustion and Ground Fires: Ecological Effects and Multi-Scale Significance. *Fire Ecology* **2013**, *9* (1), 124−132.
(52) Smith, D. M.; Cui, T.; Fiddler, M. N.; Pokhrel, R.; Surratt, J. D.; Bililign, S. Laboratory studies of fresh and aged biomass burning aerosols emitted from east African biomass fuels - Part 2: Chemical properties and characterization. *Atmos. Chem. Phys.* **2020**, *20* (17), 10169−10191.
(53) Moschos, V.; Christensen, C.; Mouton, M.; Fiddler, M. N.; Isolabella, T.; Mazzei, F.; Massabò, D.; Turpin, B. J.; Bililign, S.; Surratt, J. D. Quantifying the Light-Absorption Properties and Molecular Composition of Brown Carbon Aerosol from Sub-Saharan African Biomass Combustion. *Environ. Sci. Technol.* **2024**, *58* (9), 4268−4280.
(54) Mouton, M.; Malek, K. A.; James, M. S. H.; Pokhrel, R. P.; Fiddler, M. N.; Asa-Awuku, A. A.; Bililign, S. The hygroscopic properties of biomass burning aerosol from Eucalyptus and cow dung under different combustion conditions. *Aerosol Sci. Technol.* **2023**, *57* (7), 665−677.
(55) Bewket, W. Biofuel Consumption, Household Level Tree Planting and Its Implications for Environmental Management in the Northwestern Highlands of Ethiopia. *Eastern Africa Social Science Research Review* **2005**, *21* (1), 19−38.
(56) Urbanski, S. Wildland fire emissions, carbon, and climate: Emission factors. *Forest Ecology and Management* **2014**, *317*, 51−60.
(57) Czech, H.; Sippula, O.; Kortelainen, M.; Tissari, J.; Radischat, C.; Passig, J.; Streibel, T.; Jokiniemi, J.; Zimmermann, R. On-line analysis of organic emissions from residential wood combustion with single-photon ionisation time-of-flight mass spectrometry (SPI-TOFMS). *Fuel* **2016**, *177*, 334−342.
(58) Evans, R. L.; Bryant, D. J.; Voliotis, A.; Hu, D.; Wu, H.; Syafira, S. A.; Oghama, O. E.; McFiggans, G.; Hamilton, J. F.; Rickard, A. R. The importance of burning conditions on the composition of domestic biomass burning organic aerosol and the impact of atmospheric aging. *EGUsphere* **2024**, *2024*, 1−38.
(59) Andreae, M. O.; Merlet, P. Emission of trace gases and aerosols from biomass burning. *Global Biogeochemical Cycles* **2001**, *15* (4), 955−966.
(60) Liu, W.-J.; Li, W.-W.; Jiang, H.; Yu, H.-Q. Fates of Chemical Elements in Biomass during Its Pyrolysis. *Chem. Rev.* **2017**, *117* (9), 6367−6398.
(61) Campbell, J. H., Fawcett, J. E.; Godwin, D. R.; Boby, L. A. *Smoke Management Guidebook for Prescribed Burning in the Southern Region*; University of Georgia Warnell School of Forestry and Natural Resources, 2020.
(62) Ward, D. E.; Hardy, C. C. Smoke emissions from wildland fires. *Environ. Int.* **1991**, *17* (2), 117−134.
(63) Stefenelli, G.; Jiang, J.; Bertrand, A.; Bruns, E. A.; Pieber, S. M.; Baltensperger, U.; Marchand, N.; Aksoyoglu, S.; Prévôt, A. S. H.; Slowik, J. G.; El Haddad, I. Secondary Organic Aerosol Formation from Smoldering and Flaming Combustion of Biomass: A Box Model Parametrization Based on Volatility Basis Set. *Atmos. Chem. Phys.* **2019**, *19* (17), 11461−11484.
(64) Stockwell, C. E.; Yokelson, R.; Kreidenweis, S. M.; Robinson, A. L.; DeMott, P. J.; Sullivan, R. C.; Reardon, J.; Ryan, K. C.; Griffith, D. W. T.; Stevens, L. Trace gas emissions from combustion of peat, crop residue, domestic biofuels, grasses, and other fuels: Configuration and Fourier transform infrared (FTIR) component of the Fourth Fire Lab at Missoula Experiment (FLAME-4). *Atmos. Chem. Phys.* **2014**, *14*, 9727.
(65) Pokhrel, R. P.; Gordon, J.; Fiddler, M. N.; Bililign, S. Impact of Combustion Conditions on Physical and Morphological Properties of Biomass Burning Aerosol. *Aerosol Sci. Technol.* **2021**, *55* (1), 80−91.
(66) US Department of Commerce, National Oceanic and Atmospheric Administration (NOAA), National Weather Service, *Discussion of Humidity*, Louisville, KY. https://www.weather.gov/lmk/humidity.
(67) Elovitz, K. M. Practical guide: Understanding what humidity does and why. *ASHRAE Journal* **1999**, *41* (4), 84−90.
(68) Hatch, L. E.; Rivas-Ubach, A.; Jen, C. N.; Lipton, M.; Goldstein, A. H.; Barsanti, K. C. Measurements of I/SVOCs in biomass-burning smoke using solid-phase extraction disks and two-dimensional gas chromatography. *Atmos. Chem. Phys.* **2018**, *18* (24), 17801−17817.
(69) Chen, Y.; Bond, T. C. Light absorption by organic carbon from wood combustion. *Atmos. Chem. Phys.* **2010**, *10* (4), 1773−1787.
(70) Cheng, Y.; He, K.-b.; Du, Z.-y.; Engling, G.; Liu, J.-m.; Ma, Y.-l.; Zheng, M.; Weber, R. J. The characteristics of brown carbon aerosol during winter in Beijing. *Atmos. Environ.* **2016**, *127*, 355−364.
(71) Surratt, J. D.; Murphy, S. M.; Kroll, J. H.; Ng, N. L.; Hildebrandt, L.; Sorooshian, A.; Szmigielski, R.; Vermeylen, R.; Maenhaut, W.; Claeys, M.; et al. Chemical Composition of Secondary Organic Aerosol Formed from the Photooxidation of Isoprene. *J. Phys. Chem. A* **2006**, *110* (31), 9665−9690.
(72) Surratt, J. D.; Chan, A. W. H.; Eddingsaas, N. C.; Chan, M.; Loza, C. L.; Kwan, A. J.; Hersey, S. P.; Flagan, R. C.; Wennberg, P. O.; Seinfeld, J. H. Reactive intermediates revealed in secondary organic aerosol formation from isoprene. *Proc. Natl. Acad. Sci. U. S. A.* **2010**, *107* (15), 6640−6645.
(73) Sengupta, D.; Samburova, V.; Bhattarai, C.; Watts, A. C.; Moosmüller, H.; Khlystov, A. Y. Polar semivolatile organic compounds in biomass-burning emissions and their chemical transformations during aging in an oxidation flow reactor. *Atmos. Chem. Phys.* **2020**, *20* (13), 8227−8250.
(74) Simoneit, B. R. T.; Schauer, J. J.; Nolte, C. G.; Oros, D. R.; Elias, V. O.; Fraser, M. P.; Rogge, W. F.; Cass, G. R. Levoglucosan, a tracer for cellulose in biomass burning and atmospheric particles. *Atmos. Environ.* **1999**, *33* (2), 173−182.
(75) Li, W.; Ge, P.; Chen, M.; Tang, J.; Cao, M.; Cui, Y.; Hu, K.; Nie, D. Tracers from Biomass Burning Emissions and Identification of Biomass Burning. *Atmosphere* **2021**, *12* (11), 1401.

https://doi.org/10.1021/acsestair.4c00206
ACS EST Air XXXX, XXX, XXX−XXX

(76) Verma, S. K.; Kawamura, K.; Chen, J.; Fu, P.; Zhu, C. Thirteen years of observations on biomass burning organic tracers over Chichijima Island in the western North Pacific: An outflow region of Asian aerosols. *J. Geophys. Res.: Atmos.* **2015**, *120* (9), 4155−4168.
(77) Vincenti, B.; Paris, E.; Carnevale, M.; Palma, A.; Guerriero, E.; Borello, D.; Paolini, V.; Gallucci, F. Saccharides as Particulate Matter Tracers of Biomass Burning: A Review. *International Journal of Environmental Research and Public Health* **2022**, *19* (7), 4387.
(78) Jen, C. N.; Liang, Y.; Hatch, L. E.; Kreisberg, N. M.; Stamatis, C.; Kristensen, K.; Battles, J. J.; Stephens, S. L.; York, R. A.; Barsanti, K. C.; et al. High Hydroquinone Emissions from Burning Manzanita. *Environ. Sci. Technol. Lett.* **2018**, *5* (6), 309−314.
(79) Alberts, B.; Johnson, A.; Lewis, J.; Raff, M.; Roberts, K.; Walter, P. *Mol. Biol. Cell*; Garland Science, 2002.
(80) Bach, L.; Faure, J.-D. Role of very-long-chain fatty acids in plant development, when chain length does matter. *Comptes Rendus. Biologies* **2010**, *333* (4), 361−370.
(81) Finewax, Z.; de Gouw, J. A.; Ziemann, P. J. Identification and Quantification of 4-Nitrocatechol Formed from OH and NO3 Radical-Initiated Reactions of Catechol in Air in the Presence of NOx: Implications for Secondary Organic Aerosol Formation from Biomass Burning. *Environ. Sci. Technol.* **2018**, *52* (4), 1981−1989.
(82) Dai, J.; Mumper, R. J. Plant Phenolics: Extraction, Analysis and Their Antioxidant and Anticancer Properties. *Molecules* **2010**, *15* (10), 7313−7352.
(83) Maria de Lourdes Reis, G. Food Phenolic Compounds: Main Classes, Sources and Their Antioxidant Power. In *Oxidative Stress and Chronic Degenerative Diseases*, Moralez-Gonzalez, J., Ed.; IntechOpen, 2013; Ch. 4.
(84) Yoshikawa, T.; Yagi, T.; Shinohara, S.; Fukunaga, T.; Nakasaka, Y.; Tago, T.; Masuda, T. Production of phenols from lignin via depolymerization and catalytic cracking. *Fuel Process. Technol.* **2013**, *108*, 69−75.
(85) Liu, Q.; Luo, L.; Zheng, L. Lignins: Biosynthesis and Biological Functions in Plants. *International Journal of Molecular Sciences* **2018**, *19* (2), 335.
(86) McGrath, T. E.; Brown, A. P.; Meruva, N. K.; Chan, W. G. Phenolic compound formation from the low temperature pyrolysis of tobacco. *Journal of Analytical and Applied Pyrolysis* **2009**, *84* (2), 170−178.
(87) Giner, R. M.; Ríos, J. L.; Máñez, S. Antioxidant Activity of Natural Hydroquinones. *Antioxidants* **2022**, *11* (2), 343.
(88) Slade, J. H.; Knopf, D. A. Heterogeneous OH oxidation of biomass burning organic aerosol surrogate compounds: assessment of volatilisation products and the role of OH concentration on the reactive uptake kinetics. *Phys. Chem. Chem. Phys.* **2013**, *15* (16), 5898−5915.
(89) Costa, M. S.; Rego, A.; Ramos, V.; Afonso, T. B.; Freitas, S.; Preto, M.; Lopes, V.; Vasconcelos, V.; Magalhães, C.; Leão, P. N. The conifer biomarkers dehydroabietic and abietic acids are widespread in Cyanobacteria. *Sci. Rep.* **2016**, *6* (1), 23436.
(90) Becker, J.; Wittmann, C. A field of dreams: Lignin valorization into chemicals, materials, fuels, and health-care products. *Biotechnology Advances* **2019**, *37* (6), 107360.
(91) Neiva, D. M.; Rencoret, J.; Marques, G.; Gutiérrez, A.; Gominho, J.; Pereira, H.; del Río, J. C. Lignin from Tree Barks: Chemical Structure and Valorization. *ChemSusChem* **2020**, *13* (17), 4537−4547.
(92) Loebel Roson, M.; Duruisseau-Kuntz, R.; Wang, M.; Klimchuk, K.; Abel, R. J.; Harynuk, J. J.; Zhao, R. Chemical Characterization of Emissions Arising from Solid Fuel Combustion—Contrasting Wood and Cow Dung Burning. *ACS Earth Space Chem.* **2021**, *5* (10), 2925−2937.
(93) Cao, F.; Zhang, S.-C.; Kawamura, K.; Liu, X.; Yang, C.; Xu, Z.; Fan, M.; Zhang, W.; Bao, M.; Chang, Y.; et al. Chemical characteristics of dicarboxylic acids and related organic compounds in PM2.5 during biomass-burning and non-biomass-burning seasons at a rural site of Northeast China. *Environ. Pollut.* **2017**, *231*, 654−662.
(94) Yang, L.; Nguyen, D. M.; Jia, S.; Reid, J. S.; Yu, L. E. Impacts of biomass burning smoke on the distributions and concentrations of C2-C5 dicarboxylic acids and dicarboxylates in a tropical urban environment. *Atmos. Environ.* **2013**, *78*, 211−218.
(95) Kundu, S.; Kawamura, K.; Andreae, T. W.; Hoffer, A.; Andreae, M. O. Molecular distributions of dicarboxylic acids, ketocarboxylic acids and α-dicarbonyls in biomass burning aerosols: implications for photochemical production and degradation in smoke layers. *Atmos. Chem. Phys.* **2010**, *10* (5), 2209−2225.
(96) Li, W.; Wang, J.; Qi, L.; Yu, W.; Nie, D.; Shi, S.; Gu, C.; Ge, X.; Chen, M. Molecular characterization of biomass burning tracer compounds in fine particles in Nanjing, China. *Atmos. Environ.* **2020**, *240*, 117837.
(97) Iinuma, Y.; Brüggemann, E.; Gnauk, T.; Müller, K.; Andreae, M. O.; Helas, G.; Parmar, R.; Herrmann, H. Source characterization of biomass burning particles: The combustion of selected European conifers, African hardwood, savanna grass, and German and Indonesian peat. *J. Geophys. Res. Atmos.* **2007**, *112* (D8), D08209.
(98) Fleming, L. T.; Lin, P.; Roberts, J. M.; Selimovic, V.; Yokelson, R.; Laskin, J.; Laskin, A.; Nizkorodov, S. A. Molecular composition and photochemical lifetimes of brown carbon chromophores in biomass burning organic aerosol. *Atmos. Chem. Phys.* **2020**, *20* (2), 1105−1129.
(99) Orwa, C. M. A.; Kindt, R.; Jamnadass, R.; Simons, A. *Agroforestree Database: a tree reference and selection guide version 4.0*; World Agroforestry Centre: Kenya, 2009.
(100) Jen, C. N.; Hatch, L. E.; Selimovic, V.; Yokelson, R. J.; Weber, R.; Fernandez, A. E.; Kreisberg, N. M.; Barsanti, K. C.; Goldstein, A. H. Speciated and total emission factors of particulate organics from burning western US wildland fuels and their dependence on combustion efficiency. *Atmos. Chem. Phys.* **2019**, *19* (2), 1013−1026.
(101) Hosseini, S.; Urbanski, S. P.; Dixit, P.; Qi, L.; Burling, I. R.; Yokelson, R. J.; Johnson, T. J.; Shrivastava, M.; Jung, H. S.; Weise, D. R.; et al. Laboratory characterization of PM emissions from combustion of wildland biomass fuels. *Journal of Geophysical Research: Atmospheres* **2013**, *118* (17), 9914−9929.
(102) Burling, I. R.; Yokelson, R. J.; Griffith, D. W. T.; Johnson, T. J.; Veres, P.; Roberts, J. M.; Warneke, C.; Urbanski, S. P.; Reardon, J.; Weise, D. R.; et al. Laboratory measurements of trace gas emissions from biomass burning of fuel types from the southeastern and southwestern United States. *Atmos. Chem. Phys.* **2010**, *10* (22), 11115−11130.
(103) Rundel, P. W.; Arroyo, M. T. K.; Cowling, R. M.; Keeley, J. E.; Lamont, B. B.; Vargas, P. Mediterranean Biomes: Evolution of Their Vegetation, Floras, and Climate. *Annual Review of Ecology, Evolution, and Systematics* **2016**, *47*, 383−407.
(104) Jimenez, J. L.; Canagaratna, M. R.; Donahue, N. M.; Prevot, A. S. H.; Zhang, Q.; Kroll, J. H.; DeCarlo, P. F.; Allan, J. D.; Coe, H.; Ng, N. L.; et al. Evolution of Organic Aerosols in the Atmosphere. *Science* **2009**, *326* (5959), 1525−1529.
(105) Kessler, S. H.; Smith, J. D.; Che, D. L.; Worsnop, D. R.; Wilson, K. R.; Kroll, J. H. Chemical Sinks of Organic Aerosol: Kinetics and Products of the Heterogeneous Oxidation of Erythritol and Levoglucosan. *Environ. Sci. Technol.* **2010**, *44* (18), 7005−7010.
(106) Bai, J.; Sun, X.; Zhang, C.; Xu, Y.; Qi, C. The OH-initiated atmospheric reaction mechanism and kinetics for levoglucosan emitted in biomass burning. *Chemosphere* **2013**, *93* (9), 2004−2010.
(107) Li, J.; Forrester, S. M.; Knopf, D. A. Heterogeneous oxidation of amorphous organic aerosol surrogates by O3, NO3, and OH at typical tropospheric temperatures. *Atmos. Chem. Phys.* **2020**, *20* (10), 6055−6080.
(108) Slade, J. H.; Knopf, D. A. Multiphase OH oxidation kinetics of organic aerosol: The role of particle phase state and relative humidity. *Geophys. Res. Lett.* **2014**, *41* (14), 5297−5306.
(109) Kawamoto, H. Lignin pyrolysis reactions. *Journal of Wood Science* **2017**, *63* (2), 117−132.
(110) Liu, C.; He, Y.; Chen, X. e. Kinetic study on the heterogeneous degradation of coniferyl alcohol by OH radicals. *Chemosphere* **2020**, *241*, 125088.

https://doi.org/10.1021/acsestair.4c00206
ACS EST Air XXXX, XXX, XXX−XXX

(111) Fredrickson, C. D.; Palm, B. B.; Lee, B. H.; Zhang, X.; Orlando, J. J.; Tyndall, G. S.; Garofalo, L. A.; Pothier, M. A.; Farmer, D. K.; Decker, Z. C. J.; et al. Formation and Evolution of Catechol-Derived SOA Mass, Composition, Volatility, and Light Absorption. *ACS Earth Space Chem.* **2022**, *6* (4), 1067−1079.
(112) Pillar-Little, E. A.; Zhou, R.; Guzman, M. I. Heterogeneous Oxidation of Catechol. *J. Phys. Chem. A* **2015**, *119* (41), 10349−10359.
(113) Cubison, M. J.; Ortega, A. M.; Hayes, P. L.; Farmer, D. K.; Day, D.; Lechner, M. J.; Brune, W. H.; Apel, E.; Diskin, G. S.; Fisher, J. A.; et al. Effects of aging on organic aerosol from open biomass burning smoke in aircraft and laboratory studies. *Atmos. Chem. Phys.* **2011**, *11* (23), 12049−12064.
(114) Yang, C.; Zhang, C.; Luo, X.; Liu, X.; Cao, F.; Zhang, Y.-l. Isomerization and Degradation of Levoglucosan via the Photo-Fenton Process: Insights from Aqueous-Phase Experiments and Atmospheric Particulate Matter. *Environ. Sci. Technol.* **2020**, *54* (19), 11789−11797.
(115) Janoszka, K.; Czaplicka, M. Correlation Between Biomass Burning Tracers in Urban and Rural Particles in Silesia—Case Study. *Water, Air, & Soil Pollution* **2022**, *233* (2), 62.
(116) Li, R.; Zhang, K.; Li, Q.; Yang, L.; Wang, S.; Liu, Z.; Zhang, X.; Chen, H.; Yi, Y.; Feng, J.; et al. Characteristics and degradation of organic aerosols from cooking sources based on hourly observations of organic molecular markers in urban environments. *Atmos. Chem. Phys.* **2023**, *23* (5), 3065−3081.
(117) Gonçalves, S.; Mansinhos, I.; Romano, A. Chapter 11 - Aromatic plants: A source of compounds with antioxidant and neuroprotective effects. In *Oxidative Stress and Dietary Antioxidants in Neurological Diseases*, Martin, C. R.; Preedy, V. R., Eds.; Academic Press, 2020; pp 155−173.
(118) Chen, X.; Hopke, P. K. A chamber study of secondary organic aerosol formation by linalool ozonolysis. *Atmos. Environ.* **2009**, *43* (25), 3935−3940.
(119) Lee, A.; Goldstein, A. H.; Kroll, J. H.; Ng, N. L.; Varutbangkul, V.; Flagan, R. C.; Seinfeld, J. H. Gas-phase products and secondary aerosol yields from the photooxidation of 16 different terpenes. *J. Geophys. Res.: Atmos.* **2006**, *111* (D17), D17305.
(120) Chen, X.; Hopke, P. K.; Carter, W. P. L. Secondary Organic Aerosol from Ozonolysis of Biogenic Volatile Organic Compounds: Chamber Studies of Particle and Reactive Oxygen Species Formation. *Environ. Sci. Technol.* **2011**, *45* (1), 276−282.
(121) Hoffmann-Ostenhof, O.; Pittner, F. The biosynthesis of myo-inositol and its isomers. *Can. J. Chem.* **1982**, *60* (14), 1863−1871.
(122) Clemente, Á.; Yubero, E.; Nicolás, J. F.; Crespo, J.; Galindo, N. Organic tracers in fine and coarse aerosols at an urban Mediterranean site: contribution of biomass burning and biogenic emissions. *Environmental Science and Pollution Research* **2024**, *31* (17), 25216−25226.
(123) Marynowski, L.; Łupikasza, E.; Dąbrowska-Zapart, K.; Małarzewski, Ł.; Niedźwiedź, T.; Simoneit, B. R. T. Seasonal and vertical variability of saccharides and other organic tracers of PM_{10} in relation to weather conditions in an urban environment of Upper Silesia, Poland. *Atmos. Environ.* **2020**, *242*, 117849.
(124) Azab, A. D-Pinitol—Active Natural Product from Carob with Notable Insulin Regulation. *Nutrients* **2022**, *14* (7), 1453.
(125) Bates, S. H.; Jones, R. B.; Bailey, C. J. Insulin-like effect of pinitol. *Br. J. Pharmacol.* **2000**, *130* (8), 1944−1948.
(126) Gao, Y.; Zhang, M.; Wu, T.; Xu, M.; Cai, H.; Zhang, Z. Effects of d-Pinitol on Insulin Resistance through the PI3K/Akt Signaling Pathway in Type 2 Diabetes Mellitus Rats. *J. Agric. Food Chem.* **2015**, *63* (26), 6019−6026.
(127) Ignacio López-Sánchez, J.; Moreno, D. A.; García-Viguer, C. D-pinitol, a highly valuable product from carob pods: Health-promoting effects and metabolic pathways of this natural super-food ingredient and its derivatives. *AIMS Agriculture and Food* **2018**, *3* (1), 41−63.
(128) Poongothai, G.; et al. A review on insulinomimetic pinitol from plants. *International Journal of Pharma and Bio Sciences* **2013**, *4* (2), 992−1009.
(129) Medeiros, P. M.; Simoneit, B. R. T. Source Profiles of Organic Compounds Emitted upon Combustion of Green Vegetation from Temperate Climate Forests. *Environ. Sci. Technol.* **2008**, *42* (22), 8310−8316.
(130) Seo, S.-M.; Jeong, Y.-S.; Hari, D. K.; Shin, D.-H.; Lee, I.-J.; Park, E.-S.; Lee, J.-D.; Hwang, Y.-H. Variation of Pinitol Content for Domestic Legume Species in Korea. *Korean Journal of Crop Science* **2011**, *56* (1), 50−56.
(131) Koekemoer, M.; Steyn, H. M.; Bester, S. P. *Guide to Plant Families of Southern Africa Strelitzia 31*, ed. 2; 2014, South African National Biodiversity Institute, Pretoria.
(132) GBIF. *GBIF Backbone Taxonomy. Checklist dataset*, 2023.
(133) Smith, A. E.; Phillips, D. V. Occurrence of Pinitol in Foliage of Several Forage Legume Species1. *Crop Science* **1980**, *20* (1), 75−77.
(134) Hennigan, C. J.; Sullivan, A. P.; Collett, J. L., Jr; Robinson, A. L. Levoglucosan stability in biomass burning particles exposed to hydroxyl radicals. *Geophys. Res. Lett.* **2010**, *37*, L09806.
(135) Kalogridis, A. C.; Popovicheva, O. B.; Engling, G.; Diapouli, E.; Kawamura, K.; Tachibana, E.; Ono, K.; Kozlov, V. S.; Eleftheriadis, K. Smoke aerosol chemistry and aging of Siberian biomass burning emissions in a large aerosol chamber. *Atmos. Environ.* **2018**, *185*, 15−28.

https://doi.org/10.1021/acsestair.4c00206
ACS EST Air XXXX, XXX, XXX−XXX